Extensive numerical study of a D-brane, anti-D-brane system in AdS_5/CFT_4

Árpád Hegedűs

Wigner Research Centre for Physics,
H-1525 Budapest 114, P.O.B. 49, Hungary

Abstract

In this paper the hybrid-NLIE approach of [38] is extended to the ground state of a D-brane anti-D-brane system in AdS/CFT. The hybrid-NLIE equations presented in the paper are finite component alternatives of the previously proposed TBA equations and they admit an appropriate framework for the numerical investigation of the ground state of the problem. Straightforward numerical iterative methods fail to converge, thus new numerical methods are worked out to solve the equations. Our numerical data confirm the previous TBA data. In view of the numerical results the mysterious $L = 1$ case is also commented in the paper.

1 Introduction

In this paper in the context of AdS/CFT [1, 2, 3] we study numerically the ground state of a pair of open strings stretching between two coincident $D3$-branes with opposite orientations in S^5 of $AdS_5 \times S^5$. The main motivation for the study is that according to string-theory the ground state of such a configuration is expected to be tachyonic for large values of the 't Hooft coupling [4]. In our work we rely on the perturbatively discovered and later "all loop conjectured" integrability [5] of both the $AdS_5 \times S^5$ super-string and the dual large N gauge theory. For string configurations with D-branes integrability enabled one to describe string configurations ending on different types of D-branes as 1-dimensional integrable scattering theories with boundaries [6, 7, 8, 9, 10]. This formulation of the problem makes it possible to go beyond the approaches of perturbative gauge and string theories being valid for small and large values of the 't Hooft coupling respectively, and to determine the exact spectrum of the model at any value of the coupling constant. However, even with the help of the powerful techniques offered by integrability, the exact analytical solution of the problem is not possible. Remarkeble analytical results are available in the small [11, 12, 13, 14, 15, 32] and large [16, 17, 19, 18] coupling regimes, but the determination of the spectrum at any value of the coupling constant can only be carried out by high precision numerical solution [20, 21, 22] of the corresponding nonlinear integral equations.

In our paper we consider the case, when the two $D3$-branes are giant gravitons [23], namely they carry N units of angular momenta in S^5. If the S^5 of $AdS_5 \times S^5$ is parametrized by three complex coordinates X, Y, Z satisfying the constraint: $|X|^2 + |Y|^2 + |Z|^2 = 1$, then our $D3$-brane and anti-$D3$-brane are given by the conditions $Y = 0$ and $\bar{Y} = 0$ respectively. They wrap the same S^3, but with opposite orientation. As a consequence of Gauss law such a system can support only even number of open strings. For this reason we study the minimal number of allowed open strings, a single pair, ending on our D-brane anti-D-brane ($D\bar{D}$) system with open string angular momenta L and L'.

On the large N gauge theory side a $Y = 0$ brane is represented by a determinant operator [24] composed of N copies of the field Y:

$$\mathcal{O}_Y = \det Y = \epsilon^{a_1 \cdots a_N}_{b_1 \cdots b_N} Y^{b_1}_{a_1} \cdots Y^{b_N}_{a_N} \tag{1.1}$$

where a_i and b_i are color indices and ϵ is a product of two regular epsilon tensors $\epsilon_{b_1 \cdots b_N}^{a_1 \cdots a_N} = \epsilon^{a_1 \cdots a_N} \epsilon_{b_1 \cdots b_N}$. The local operator corresponding to an open string ending on a $Y = 0$ giant graviton can be obtained from (1.1) by replacing one Y field with an adjoint valued operator $\mathcal{W}$ [25]:

$$\mathcal{O}_Y^{\mathcal{W}} = \epsilon_{b_1 \cdots b_N}^{a_1 \cdots a_N} Y_{a_1}^{b_1} \cdots Y_{a_{N-1}}^{b_{N-1}} \mathcal{W}_{a_N}^{b_N} . \tag{1.2}$$

The gauge theory description of a pair of open strings stretching between two D-branes is given by a double determinant operator, such that the string insertions $\mathcal{W}$ and $\mathcal{V}$ connect the two determinants of the Y fields[1]:

$$\mathcal{O}_{Y,Y}^{\mathcal{W},\mathcal{V}} = \epsilon_{b_1 \cdots b_N}^{a_1 \cdots a_N} Y_{a_1}^{b_1} \cdots Y_{a_{N-1}}^{b_{N-1}} \epsilon_{d_1 \cdots d_N}^{c_1 \cdots c_N} Y_{c_1}^{d_1} \cdots Y_{c_{N-1}}^{d_{N-1}} \mathcal{W}_{a_N}^{d_N} \mathcal{V}_{c_N}^{b_N} \tag{1.3}$$

Unfortunately, the precise gauge theory dual of the $D\bar{D}$-system of our interest is not known. In [4] it was approximated by a double determinant operator similar to (1.3), but in one of the determinants the Y fields are replaced with $\bar{Y}$ fields[2]:

$$\mathcal{O}_{Y\bar{Y}}^{\mathcal{W},\mathcal{V}} = \epsilon_{b_1 \cdots b_N}^{a_1 \cdots a_N} Y_{a_1}^{b_1} \cdots Y_{a_{N-1}}^{b_{N-1}} \epsilon_{d_1 \cdots d_N}^{c_1 \cdots c_N} \bar{Y}_{c_1}^{d_1} \cdots \bar{Y}_{c_{N-1}}^{d_{N-1}} \mathcal{W}_{a_N}^{d_N} \mathcal{V}_{c_N}^{b_N} . \tag{1.4}$$

For the ground state the insertions are $\mathcal{W} = Z^L$ and $\mathcal{V} = Z^{L'}$ respectively. Based on one-loop results the planar dilatation operator is expected to act independently on the two words $\mathcal{W}, \mathcal{V}$ corresponding to the open string states [4]:

$$\Delta[\mathcal{O}_{Y\bar{Y}}^{\mathcal{W},\mathcal{V}}] = \Delta_{\text{bare}}[\mathcal{O}_{Y\bar{Y}}^{\mathcal{W},\mathcal{V}}] + \delta\Delta[\mathcal{W}_{Y\bar{Y}}] + \delta\Delta[\mathcal{V}_{\bar{Y}Y}]. \tag{1.5}$$

This observation allows us to apply the boundary Thermodynamic Bethe Ansatz technique (BTBA) [26] to each open string separately. The necessary ingredients of this technique are the boundary reflection factors [8, 27, 28, 29] and the asymptotic Bethe equations of the problem [4]. Unfortunately, apart from some very special cases [30, 31, 32], it is still unknown how to derive BTBA equations for a general non-diagonal scattering theory in the context of the thermodynamical considerations of [26]. This is why in [4] the Y-system [33, 34, 35] and the related discontinuity [36]

---

[1]The ground state of such string states is BPS.

[2]According to the argument of [4] the correct state might have other structures involving the fields Y and $\bar{Y}$, but should be similar to the double determinant form (1.4) and the mixing with other fields seem to be suppressed at large N

equations supplemented by analyticity assumptions compatible with the asymptotic solution [37] were used to derive BTBA equations for the nonperturbative study of the ground state of the $D\bar{D}$-system [4].

The BTBA description of the system is an infinite set of nonlinear integral equations. The numerical solution of the equations [4] showed that the ground state energy is a monotonously decreasing function of the coupling constant[3] g. The analytical investigation of the large rapidity and large index behavior of the Y-functions of the BTBA revealed that the usual BTBA description of the system breaks down when the energy of an open string state with angular momentum L gets close to the critical value: $E_c(L) = 1 - L$. This point was interpreted in [4] as a transition point where the ground state becomes tachyonic. Approaching the critical point the contribution of infinitely many Y-functions must be taken into account to get accurate numerical result for the energy[4]. This fact suggests reformulating the finite size problem in terms of finite number of unknown functions. The possible candidates could be the FiNLIE [46], the quantum spectral curve (QSC) [47, 48] or the hybrid-NLIE (HNLIE) [38] formulation of the problem. Since at present it is not known (not even for the Konishi problem) how to use the analytically very efficient [19, 14] QSC method for numerical purposes, we choose the HNLIE method to reformulate the finite size problem of the $D\bar{D}$-system. In this paper we transformed the infinite set of boundary TBA equations [4] into a finite set of hybrid-NLIE type of nonlinear integral equations. We perform the extensive numerical study of these type of equations in order to get as close to the special $E_{BTBA} = 1 - L$ critical point as it is possible.

Our numerical results reproduce the numerical evaluation of the boundary Lüscher formula [27, 39] in the linear approximation, and the numerical BTBA results of [4] as well. These numerical comparisons give further numerical checks on the hybrid-NLIE technique of [38]. Unfortunately, as g increases new local singularities enter the HNLIE formulation of the problem. Thus we could not approach very close to the critical point. Nevertheless, in the range of g where physically acceptable numer-

---

[3]Throughout the paper the relation between g and the 't Hooft coupling λ is given by: $\lambda = 4\pi^2 g^2$.

[4]This means that the usual truncation procedure for solving the infinite set of TBA equations is not applicable to such a system

ical results were obtained, the HNLIE results could give higher numerical precision than that of the BTBA and also some interesting facts could be read off from our numerical data.

During the numerical solution of the HNLIE equations straightforward numerical iterative methods failed to converge, thus new numerical methods were worked out to solve the equations.

The ground state of the $L = 1$ state is a very special case, since there the critical point is right at $g = 0$ and so far neither perturbative field theory computations nor the boundary Lüscher formula could provide a finite quantitative answer to the anomalous dimension of this state. On the integrability side the HNLIE approach allows us to get some numerical insight into this problem.

The outline of the paper is as follows: Section 2. contains the HNLIE equations. In section 3. the numerical method is described. In section 4. the numerical results and their interpretation is presented. Section 5. contains some comments on the mysterious $L = 1$ case and finally our conclusion is given in section 6. Various notations, kernels of the integral equations together with the necessary asymptotic solutions are placed in the appendices of the paper.

2 The HNLIE equations

In this section we transform the previously proposed BTBA equations of [4] for the ground state of our D-brane anti-D-brane system to finite component hybrid-NLIE equations. For presentational purposes we group the equations into 3 types. There are TBA-type equations, horizontal $SU(2)$ hybrid-NLIE type equations, and vertical $SU(4)$ hybrid-NLIE type equations. They together form a closed set of non-linear integral-equations, which are solved numerically in this paper. As it is usual, structurally the equations consist of source terms plus convolutions containing coupling dependent kernels and nonlinear combinations of the unknown functions. The objects appearing in the arguments of the source functions are subjected to quantization conditions, but similarly to the boundary TBA description [4], due to the $u \to -u$ symmetry of the problem they are tied to the origin of the complex plane, thus extra quantization conditions are unnecessary to be imposed, since they are automatically satisfied by symmetry. Since these source term objects have fixed

positions their positions are exactly the same as that of their asymptotic counterparts. This fact saves us from the tedious computation of the source terms, since if we take the difference of the exact equations and their asymptotic counterparts the source terms cancel from the equations. To be pragmatic and save time and space, the equations will be presented in such a difference form. Thus for any combination f of the unknown functions, we introduce the notation $\delta f(u) = f(u) - f^o(u)$, where $f^o(u)$ is the asymptotic counterpart of f. Having introduced this notation, we start the presentation of the equations by the TBA-type part. For the labeling of the Y-functions we use the string-hypothesis [40] based notations of [41]. For the presentation of the equations a few more notations need to be introduced:

$$\mathscr{L}_{\pm} = \log\left[\tau^2\left(1 - \frac{1}{Y_{\pm}}\right)\right], \qquad \mathscr{L}_m = \log\left[\tau^2\left(1 + \frac{1}{Y_{m|vw}}\right)\right], \qquad \tau(u) = \tanh(\frac{\pi g u}{4}).$$

(2.1)

For later numerical purposes we re-parametrize $\log Y_Q$ by the formula:

$$\log Y_Q(u) = -2L \, \log\frac{x^{[Q]}(u)}{x^{[-Q]}(u)} + \log\bar{y}_Q(u) + c_Q + \varepsilon \, \log\left(u^2 + \frac{(Q+1)^2}{g^2}\right), \qquad Q = 1, 2, ...$$

(2.2)

such that c_Q is the constant value of $\log Y_Q$ at infinity and ε is minus twice the energy[5]: $\varepsilon = -2\,E_{BTBA}$. From the TBA equations of the problem [4], it follows that $\delta c_Q = c_Q - c_Q^o \equiv \delta c$ is Q-independent, and for small g, $\log \bar{y}_Q$ is a smooth deformation of its asymptotic counterpart, such that $\delta \log \bar{y}_Q$ tends to zero at infinity.[6]

Using this decomposition the following notations are need to be introduced:

$$L_Q = \log(1 + Y_Q), \qquad \delta R_Q = \log(1 + Y_Q) - \delta \log \bar{y}_Q.$$

(2.3)

Then the TBA-type equations take the form:

$$\delta\log Y_{m|vw} = \delta \log\left[(1 + Y_{m+1|vw})(1 + Y_{m-1|vw})\right]\star s - \log(1 + Y_{m+1})\star s, \quad 2 \leq m \leq p_0 - 2,$$

(2.4)

---

[5]The log multiplier of ε in (2.2) is chosen not to modify the constant term in the large u behavior and to satisfy $\frac{Y_Q^+ Y_Q^-}{Y_{Q-1} Y_{Q+1}} \frac{Y_{Q-1}^o Y_{Q+1}^o}{Y_Q^{o+} Y_Q^{o-}} = \frac{\bar{y}_Q^+ \bar{y}_Q^-}{\bar{y}_{Q-1} \bar{y}_{Q+1}} \frac{\bar{y}_{Q-1}^o \bar{y}_{Q+1}^o}{\bar{y}_Q^{o+} \bar{y}_Q^{o-}}$, which is the LHS of an important Y-system equation divided by its asymptotic counterpart.

[6]$\log Y_Q$ cannot be considered as smooth deformation of $\log Y_Q^o$, because $\log Y_Q - \log Y_Q^o \sim \varepsilon \log |u|$ diverges for large u at any g. On the other hand $\log \bar{y}_Q - \log \bar{y}_Q^o$ is small for any u at small g and tends to zero at infinity.

$$\delta \log Y_{1|vw} = \delta \log \left(1 + Y_{2|vw}\right) \star s - \log(1 + Y_2) \star s + \delta \log \left[\frac{1 - Y_-}{1 - Y_+}\right] \hat{\star} s, \quad (2.5)$$

$$\delta \log \bar{y}_Q = 2\,\delta \mathscr{L}_{Q-1} \star s - (\delta R_{Q-1} + \delta R_{Q+1} \star s), \quad Q \geq 2, \quad\quad (2.6)$$

$$\delta \log \frac{Y_-}{Y_+} = -\sum_{Q=1}^{p_0-2} \log(1 + Y_Q) \star K_{Qy} - \Omega(K_{Qy}). \quad\quad (2.7)$$

$$\delta\log(Y_+ Y_-) = 2\delta\log\left[\frac{1 + Y_{1|vw}}{1 + Y_{1|w}}\right] \star s + \sum_{Q=1}^{p_0-2} \log(1 + Y_Q) \star \left[-K_Q + 2K_{xv}^{Q1} \star s\right]$$
$$- \Omega(K_Q) + 2\,\Omega(K_{xv}^{Q1} \star s) \quad\quad (2.8)$$

For Y_1 the modified hybrid form [42] of the BTBA equations is used,

$$\delta\log \bar{y}_1 = 2\delta \log(1 + Y_{1|vw}) \star s \hat{\star} K_{y1}$$
$$- 2\delta \log\left[\frac{1 - Y_-}{1 - Y_+}\right] \hat{\star} s \star K_{vwx}^{11} + 2\delta\mathscr{L}_- \hat{\star} K_-^{y1} + 2\delta\mathscr{L}_+ \hat{\star} K_+^{y1}$$
$$+ \sum_{Q=1}^{p_0-2} \log(1 + Y_Q) \star \left[K_{\mathfrak{sl}(2)}^{Q1} + 2s \star K_{vwx}^{Q-1,1}\right]$$
$$+ \Omega(K_{\mathfrak{sl}(2)}^{Q1}) + 2\Omega(s \star K_{vwx}^{Q-1,1}), \quad\quad (2.9)$$

where p_0 is the index limit starting from which the upper part of the TBA equations is replaced by an $SU(4)$ NLIE of [38] (See figure 1.). For any kernel vector appearing in the TBA equations $\Omega(\mathcal{K}_Q)$ denotes the residual sum $\sum\limits_{Q=p_0-1}^{\infty} L_Q \star \mathcal{K}_Q$, and following the method of [42] for $p_0 \geq 4$ it can be expressed by next to nearest neighbor Y-functions as follows:

$$\Omega(\mathcal{K}_Q) = \delta R_{p_0-1} \star \sigma_{\frac{1}{2}} \star \mathcal{K}_{p_0-2} - \delta R_{p_0-2} \star \sigma_{\frac{1}{2}} \star \mathcal{K}_{p_0-1}$$
$$+ 2\delta r_{p_0-2} \star s_{\frac{1}{2}} \star \mathcal{K}_{p_0-2} - 2\delta r_{p_0-3} \star s_{\frac{1}{2}} \star \mathcal{K}_{p_0-1}, \quad\quad (2.10)$$

where $r_m = \log(1 + Y_{m|vw})$, the kernels $s, s_{\frac{1}{2}}, \sigma_{\frac{1}{2}}$ are hyperbolic functions [42],

$$s(u) = \frac{g}{4 \cosh \frac{\pi g u}{2}}, \qquad s_{\frac{1}{2}}(u) = \frac{1}{2} s(\frac{u}{2}), \qquad \sigma_{1/2}(u) = \frac{g}{2\sqrt{2}} \frac{\cosh \frac{\pi g u}{4}}{\cosh \frac{\pi g u}{2}}, \quad\quad (2.11)$$

while the other TBA kernels can be found in appendix A. As a consequence of the re-parametrization (2.2) the two constants δc and ε also become part of the set of

equations[7]:

$$\varepsilon = \frac{1}{2\pi}\sum_{Q=1}^{p_0-2} L_Q \star \frac{d\tilde{p}^Q}{du} + \frac{1}{2\pi}\Omega(\frac{d\tilde{p}^Q}{du}), \tag{2.12}$$

$$
\begin{aligned}
\delta c =& 2\delta \log(1+Y_{1|vw}) \star s \,\hat{\star}\, CK_{y1}\\
&- 2\delta \log\left[\frac{1-Y_-}{1-Y_+}\right] \,\hat{\star}\, s \star CK_{vwx}^{11} + 2\delta\mathscr{L}_- \,\hat{\star}\, CK_-^{y1} + 2\delta\mathscr{L}_+ \,\hat{\star}\, CK_+^{y1}\\
&+ \sum_{Q=1}^{p_0-2} \log(1+Y_Q) \star \left[CK_{\mathfrak{sl}(2)}^{Q1} + 2s \star CK_{vwx}^{Q-1,1}\right]\\
&+ \Omega(CK_{\mathfrak{sl}(2)}^{Q1}) + 2\Omega(s \star CK_{vwx}^{Q-1,1}),
\end{aligned}
\tag{2.13}
$$

where for any kernel $\mathcal{K}$: $C\mathcal{K}(u)$ denotes the constant term in the large v expansion of $\mathcal{K}(u,v)$.[8] As we mentioned $-\varepsilon/2$ is the TBA energy, thus (2.12) gives the energy formula in our formulation of the finite size problem. The asymptotic forms of the Y-functions necessary for the formulation of (2.4-2.13) are listed in appendix D. To close the discussion of the TBA-type equations we note that equations (2.7) and (2.8) determine $Y_\pm$ up to an overall sign factor. The sign factor can be fixed from the asymptotic solution and its value is -1. Thus the fermionic Y-functions can be expressed in terms of the LHS of (2.7) and (2.8) by the formula:

$$Y_{\mp} = -e^{\frac{1}{2}\log Y_+ Y_- \pm \frac{1}{2}\log \frac{Y_-}{Y_+}}. \tag{2.14}$$

The horizontal $SU(2)$ wing of the TBA is resumed by an $SU(2)$-type NLIE [43, 38], which in our case takes the form:

$$\delta\log(-b) = s^{[1-\gamma]} \star \delta \log(1+Y_{1|w}) + G \star \delta \log(-1-b) - G^{[-2\gamma]} \star \delta \log(-1-\bar{b}), \tag{2.15}$$

$$\delta \log(-\bar{b}) = s^{[\gamma-1]} \star \delta \log(1+Y_{1|w}) + G \star \delta \log(-1-\bar{b}) - G^{[2\gamma]} \star \delta \log(-1-b), \tag{2.16}$$

$$\delta\log Y_{1|w} = s^{[\gamma-1]} \star \delta\log(-1-b) + s^{[1-\gamma]} \star \delta\log(-1-\bar{b}) + \delta\log\left[\frac{1-\frac{1}{Y_-}}{1-\frac{1}{Y_+}}\right] \,\hat{\star}\, s, \tag{2.17}$$

where $0 < \gamma < 1/2$ is a contour shift parameter, the kernel G is given by (B.6) and the asymptotic solution for b and $\bar{b}$ is given in appendix D[9]. The upper $SU(4)$ NLIE

---

[7]Here the $\star$ notation means simply integration from $-\infty$ to ∞.

[8]Here we note that only the dressing kernel has logarithmically divergent term in its large v expansion, all the other kernels has either constant term or they simply vanish at infinity.

[9]In practice b and $\bar{b}$ are complex conjugate of each other.

of [38] is attached to the TBA equations at the p_0-th node. The upper NLIE is for 12 complex unknown functions: b_A and d_A, $\quad A = 1, ..., 6$. They are combinations of the T-functions of the upper wing $SU(4)$ Bäcklund-hierarchy [38]. Their relations to the unknowns introduced in [38] are given by (B.3,B.4) in appendix B and their asymptotic forms are given in appendix C. Using the notation $B_A = 1 + b_A$ and $D_A = 1 + d_A$, the equations they satisfy take the form:

$$\delta \log b_A = \sum_{A'} (G_{bB})_{AA'} \star \delta \log B_{A'} + \sum_{A'} (G_{bD})_{AA'} \star \delta \log D_{A'} + E_A, \qquad (2.18)$$

$$\delta \log d_A = \sum_{A'} (G_{dB})_{AA'} \star \delta \log B_{A'} + \sum_{A'} (G_{dD})_{AA'} \star \delta \log D_{A'} + \bar{E}_A, \qquad (2.19)$$

where the kernels are given in (B.5-B.12). The shifts in the kernels which is equivalent to fixing the lines on which the NLIE variables live, are chosen in a symmetrical way and fixed as follows:

$$\underline{\gamma} = \{\gamma_a\} = \{\gamma_1^{(3)}, \gamma_2^{(3)}, \gamma_3^{(3)}, \gamma_1^{(2)}, \gamma_2^{(2)}, \gamma_1^{(1)}\} = \frac{1}{12}(-9, -1, 5, -3, 3, 1), \qquad (2.20)$$

$$\underline{\eta} = \{\eta_a\} = \{\eta_1^{(3)}, \eta_2^{(3)}, \eta_3^{(3)}, \eta_1^{(2)}, \eta_2^{(2)}, \eta_1^{(1)}\} = \frac{1}{12}(-5, 1, 9, -3, 3, -1). \qquad (2.21)$$

This choice satisfies the constraint inequalities of [38] and satisfy the relation $\underline{\gamma} = -\mathfrak{M}\underline{\eta}$ with $\mathfrak{M}$ given by (C.21). Its advantage is that choosing the $C = 0$ asymptotic solution from appendix C to formulate the equations, the b- and d-type variables are related in a simple manner:

$$b(-u) = \mathfrak{M}d(u). \qquad (2.22)$$

In practice this reduces to half the number of $SU(4)$ NLIE variables. The vectors E_A and $\bar{E}_A$ are conjugate to each other and they give the TBA input into the upper NLIE. To give their form we introduce the notations:

$$\eta_1 = Y_{p0-1|vw}^{[\epsilon_1]}, \qquad \bar{\eta}_1 = Y_{p0-1|vw}^{[\epsilon_3]}, \qquad \epsilon_1 = -\epsilon_3 = -\frac{7}{12}, \qquad (2.23)$$

$$E_1 = s^{[\frac{5}{6}]} \star \delta \log(1 + \eta_1), \qquad E_3 = s^{[\frac{5}{6}]} \star \delta \log(1 + \bar{\eta}_1), \qquad E_5 = E_6 = 0, \qquad (2.24)$$

$$E_2 = \frac{1}{2} s^{[\frac{1}{2}]} \star \delta \log(1 + \eta_1) - \frac{1}{2} s^{[\frac{2}{3}]} \star \delta \log(1 + \bar{\eta}_1) + \varepsilon_2 + i\,\varphi_2, \qquad (2.25)$$

8

$$E_4 = -\frac{1}{2} s^{\left[\frac{1}{3}\right]} \star \delta\log(1 + \eta_1) - \frac{1}{2} s^{\left[\frac{5}{6}\right]} \star \delta\log(1 + \bar{\eta}_1) + \varepsilon_4 + i\,\varphi_4, \qquad (2.26)$$

where

$$\varepsilon_2(u) = \frac{i}{2\pi} \int\limits_0^\infty dv \; \delta R_{p_0}(v) \left\{ \frac{1}{u - v - \frac{i}{12g}} + \frac{1}{u + v - \frac{i}{12g}} \right\}, \qquad (2.27)$$

$$\varepsilon_4(u) = \frac{i}{2\pi} \int\limits_0^\infty dv \; \delta R_{p_0}(v) \left\{ \frac{1}{u - v - \frac{i}{4g}} + \frac{1}{u + v - \frac{i}{4g}} \right\}, \qquad (2.28)$$

$$\varphi_2(u) = \int\limits_{-\infty}^\infty dv \; \delta\log(1 + \eta_1(v)) \left\{ \varphi(u - v + \frac{i}{2g}) + \varphi(u + v - \frac{2\,i}{3g}) \right\}, \qquad (2.29)$$

$$\varphi_4(u) = \int\limits_{-\infty}^\infty dv \; \delta\log(1 + \eta_1(v)) \left\{ \varphi(u - v + \frac{i}{3g}) + \varphi(u + v - \frac{5\,i}{6g}) \right\}, \qquad (2.30)$$

with

$$\varphi(u) = \frac{g}{8\,\pi} \left\{ i\,\psi(\frac{1}{4} - \frac{i\,u\,g}{4}) - i\,\psi(\frac{1}{4} + \frac{i\,u\,g}{4}) - \pi\,\tanh(\frac{\pi\,g\,u}{2}) \right\}. \qquad (2.31)$$

The last set of equations gives, how the upper NLIE variables couple to the TBA part of the equations.

$$\delta\log Y_{p_0-2|vw} = s^{[-\epsilon_1]} \star \delta\log(1 + \eta_1) + s \star \delta\log(1 + Y_{p_0-3|vw}) - s \star L_{p_0-1}, \qquad (2.32)$$

$$\delta\log \eta_1 = s^{[-1+\epsilon_1-\gamma_1]} \star \delta\log B_1 + s^{[1+\epsilon_1-\eta_1]} \star \delta\log D_1 - s^{[\epsilon_1-\gamma_2]} \star \delta\log B_2$$
$$+ s^{[\epsilon_1]} \star \delta\log(1 + Y_{p_0-2|vw}) - s^{[\epsilon_1]} \star L_{p_0}, \qquad (2.33)$$

$$\delta\log \bar{\eta}_1 = s^{[-1+\epsilon_3-\gamma_3]} \star \delta\log B_3 + s^{[1+\epsilon_3-\eta_3]} \star \delta\log D_3 - s^{[\epsilon_3-\eta_2]} \star \delta\log D_2$$
$$+ s^{[\epsilon_3]} \star \delta\log(1 + Y_{p_0-2|vw}) - s^{[\epsilon_3]} \star L_{p_0}, \qquad (2.34)$$

$$\delta\log \bar{y}_{p_0} = s^{[-1-\gamma_2]} \star \left[\delta\log \bar{b}_2 - \delta\log B_2 \right] + s^{[1-\eta_2]} \star \left[\delta\log \bar{d}_2 - \delta\log D_2 \right]$$
$$+ s^{[-\gamma_3]} \star \delta\log \frac{B_3}{b_3} + s^{[-\eta_1]} \star \delta\log \frac{D_1}{d_1} + s^{[-\epsilon_1]} \star \delta\log \frac{1 + \eta_1}{\eta_1}$$
$$+ s^{[-\epsilon_3]} \star \delta\log \frac{1 + \bar{\eta}_1}{\bar{\eta}_1} - s \star \delta R_{p_0-1}, \qquad (2.35)$$

where $\bar{b}_2$ and $\bar{d}_2$ are from the re-parametrization of b_2 and d_2:

$$b_2(u) = \eta \left(\frac{1}{x_s^{[-p_0+\gamma_2]}(u)} \right)^{2L} \exp \left\{ \varepsilon \left[\log \left(u + i\,\frac{\gamma_2 - p_0 - 1}{g} \right) + i\,\frac{\pi}{2} \right] + \frac{\delta c}{2} \right\} \bar{b}_2(u), \qquad (2.36)$$

$$d_2(u) = \eta \left(\frac{1}{x_s^{[p_0+\eta_2]}(u)} \right)^{2L} \exp \left\{ \varepsilon \left[\log \left(u + i \frac{\eta_2 + p_0 + 1}{g} \right) - i \frac{\pi}{2} \right] + \frac{\delta c}{2} \right\} \bar{d}_2(u),$$

(2.37)

with $\eta = \pm 1$ being a global sign factor. Similarly to the definition of $\bar{y}_Q$, also here the benefit of using $\bar{b}_2$ and $\bar{d}_2$ is that, for small g, $\log \bar{b}_2$ and $\log \bar{d}_2$ are smooth deformations of their asymptotic counterparts, and in addition $\delta \log \bar{b}_2$ and $\delta \log \bar{d}_2$ vanishes at infinity, which is necessary for the convergence of certain integrals. The decompositions (2.36),(2.37) are chosen to be compatible with the functional relation $b_2^{[-\gamma_2]} d_2^{[-\eta_2]} = Y_{p_0}$ in ref. [38]. Equations (2.4)-(2.35) constitute our complete set of nonlinear integral equations, which governs the finite size dependence of the vacuum of our D-brane anti-D-brane system.

3   The numerical method

Here we describe our numerical method for solving the hybrid-NLIE equations presented in the previous section. During the iterative numerical solution of the equations we faced with very serious convergence problems, which forced us to work out such a method that overcomes all the difficulties emerged. Our numerical method can be applied to solve other type of nonlinear integral equations as well. The power of the method is shown by the fact that numerical convergence was reached even in such cases, when the solution was physically unacceptable.

The numerical method consist of two main steps, namely:

- Discretization of the equations

- Iterative solution.

The first step involves the discretization of the unknown functions and kernels, furthermore the discrete approximate representation of the convolutions. Having carried out the appropriate discretization of the problem, the equations are considered as large nonlinear algebraic set of equations. Thus eventually instead of integral equations we solve discrete algebraic equations. In this paper we will present two methods to solve them numerically.

3.1 Discretization of the problem

The discretization serves two goals. First it allows us to reduce the numerical problem from solving integral equations to solving algebraic equations. Second choosing the discretization points appropriately it reduces the number of degrees of freedom as much as it is possible to reach the desired numerical accuracy. In our actual numerical computation instead of u of section 2. we used the new rapidity $u \to \frac{u}{g}$, because with such a scaling almost all the rapidity difference dependent kernels become g independent. Thus for example $Y_{\pm}(u)$ will be defined in $[-2g, 2g]$. To decrease the number of discretization points the $u \to -u$ symmetry of the problem is exploited. This means that the Y-functions are to be discretized only on $[0, \infty]$ or $[0, 2g]$ and as for the NLIE variables it is enough to discretize the b- and d- type variables on $[0, \infty]$. Since we do not want to introduce any cutoff in the rapidity space first we transform the $u \in [0, \infty]$ interval to a finite interval $t \in [0, B(a)]$ through the transformation formula:

$$u(t) = a \left(\frac{B(a)}{t} - 1 \right), \qquad B(a) = 2\frac{g}{a} + 1. \tag{3.1}$$

This formula is chosen such that the branch point $2g$ corresponds to $t = 1$ for any choice of the parameter a, where a is a global scaling factor which changes from unknown to unknown. We chose the values as follows: for $Y_{1|w}$ $a = 1$, for b and $\bar{b}$ $a = 2$, for Y_Q and $Y_{Q-1|vw}$ $a = Q$, for η_1 and $\bar{\eta}_1$ $a = p_0$, and finally for the b- and d-type NLIE functions $a = p_0$. These values are chosen to preserve the smoothness[10] of the transformed functions in the finite interval. After this transformation all of our unknown functions live on a finite interval. To discretize them we used piecewise Chebyshev approximation. This means that we divide the finite interval into subintervals and on each subinterval the functions are approximated by a given order Chebyshev series. The choice of subintervals is not equidistant. The subintervals are placed more densely around the branch points, since the function $x(u/g)$, which governs the decay of the massive Y_Q-functions, has the largest change around this point. The advantage of the Chebyshev approximation is that if the function is smooth enough on the subinterval, the coefficients of the Chebyshev series decay

---

[10]In our terms the lack of smoothness would not mean discontinuity, but the presence of rapidly changing parts and peaks.

rapidly and the order of magnitude of the last coefficient allows us to estimate the numerical errors of the procedure. Now we describe the discretization method in more detail. Our functions are defined on either $[0, B(Q)]$ or on $[0, 2g]$. This is why two type of subinterval vectors are defined A_Q and $A_\pm$, such that the endpoints of the subintervals of $[0, B(Q)]$ are put into the vector A_Q and the endpoints of the subintervals of $[0, 2g]$ define $A_\pm$. Let l_k be the order of the Chebyshev approximation, then using the general rules of the Chebyshev approximation, a given function $f(t)$ is approximated in the kth subinterval $[A_{k-1}, A_k]$ as:

$$f(t) \simeq \sum_{j=1}^{l_k} c_j^{(k)} \, \hat{T}_{j-1} \left(\frac{t - \frac{1}{2}(A_k + A_{k-1})}{\frac{1}{2}(A_k - A_{k-1})} \right), \qquad t \in [A_{k-1}, A_k], \qquad (3.2)$$

where now the vector A stand for either A_Q or $A_\pm$, furthermore $\hat{T}_{j-1}$ are a slightly modified Chebyshev polynomials[11]

$$\hat{T}_j(u) = \begin{cases} T_j(u) & \text{if} \quad j \geq 1, \\ \frac{1}{2} & \text{if} \quad j = 0, \end{cases}$$

with $T_j(u)$ being the jth Chebyshev polynomial[12]. The coefficients $c_j^{(k)}$ are the Chebyshev coefficients of the function f, which can be computed from the sampling points of the Chebyshev approximation:

$$t_j^{(k)} = \frac{1}{2}(A_k - A_{k-1}) \, c^{(i)}(l_k) + \frac{1}{2}(A_k + A_{k-1}), \qquad i = 1, .., l_k \qquad (3.3)$$

by the simple formula:

$$c_j^{(k)} = \frac{2}{l_k} \sum_{j_0=1}^{l_k} f(t_{l_k-j_0+1}^{(k)}) \, \tilde{C}_{j_0,j}, \qquad (3.4)$$

where $c^{(i)}(l_k)$ are the zeros of the l_k order Chebyshev polynomial:

$$c^{(i)}(l_k) = -\cos\left[\frac{\pi}{l_k} \left(i - \frac{1}{2} \right) \right], \qquad \hat{T}_{l_k}(c^{(i)}(l_k)) = 0, \qquad i = 1, ..., l_k \qquad (3.5)$$

and $\tilde{C}_{k,i}$ is given by:

$$\tilde{C}_{k,i} = \cos\left[\frac{\pi}{l_k} \left(k - \frac{1}{2} \right) (i - 1) \right], \qquad i, k \in \{1, ..., l_k\}. \qquad (3.6)$$

---

[11] This slight modification is only to write the approximation series (3.2) in a more compact way.
[12] The Chebyshev polinomials are defined by the formula: $T_j(u) = \cos(j \arccos u), \quad j = 0, 1, 2...$

In our method the next step is to formulate the convolutions and the equations themselves in terms of the discrete values of our functions. Here will sketch the basic idea in some typical scenarios appearing in our equations. Then its application to the concrete unknowns and kernels of the problem is straightforward. If one takes the equations at the required discretized points $t_j^{(k)}$ the following typical pattern arises:

$$F(u(t_{j'}^{(k')})) \simeq \int\limits_0^\infty dv'\, L(v')\, K^S(v', u(t_{j'}^{(k')})) + \dots, \qquad (3.7)$$

where $K^S(u,v) = K(u,v) + K(-u,v)$ is the symmetrized kernel to exploit left-right symmetry of the problem for reducing to half the number of variables. $F(u(t_{j'}^{(k')}))$ is intended to modelize the variables in the left-hand side of the equations taken at the discretized points of the transformed variable t and $L(u)$ stands for some nonlinear combination of some unknown function of the equations[13]. If $L(u(t))$ is discretized by a subinterval vector A of $[0, B(a)]$, then the numerical approximation of the right hand side goes as follows;

- First the integration variable is changed from v' to t,

- then on each subinterval $L(u(t))$ is approximated by its Chebyshev series,

- finally the integration is carried out and the convolution is expressed in terms of the discretized values of $L(u(t))$.

The final approximation formula takes the form:

$$\int\limits_0^\infty dv'\, L(v')\, K^S(v', u(t_{j'}^{(k')})) \simeq \sum_{k=1}^{\mathcal{L}(A)} \sum_{j=1}^{l_k} L_{k,j} \left(\frac{2}{l_k} \sum_{j_0=1}^{l_k} \tilde{C}_{l_k-j+1,j_0}\, \mathcal{K}_{k',j'}^{k,j_0} \right), \qquad (3.8)$$

where $L_{k,j} = L(u(t_j^{(k)}))$, $\mathcal{L}(A)$ denotes the dimension of A and $\mathcal{K}_{k',j'}^{k,j}$ is the discretized convolution matrix given by the formula:

$$\mathcal{K}_{k',j'}^{k,j} = a\, B(a) \int\limits_{A_{k-1}}^{A_k} \frac{dt}{t^2}\, \hat{T}_{j-1} \left(\frac{t - \frac{1}{2}(A_k + A_{k-1})}{\frac{1}{2}(A_k - A_{k-1})} \right) K^S(u(t), u(t_{j'}^{(k')})). \qquad (3.9)$$

---

[13]For example in the TBA-part $F(u)$ can be thought of as $\log Y(u)$ and $L(u)$ can be $\log(1+Y(u))$ for any type of Y.

In this manner a convolution is reduced to a discrete matrix-vector multiplication.

The other type of typical convolution is when the integration is taken from zero to $2g$. In certain cases the function $L(u)$ has square root behavior close to the branch points[14]. For such functions the truncated Chebyshev series does not give accurate approximation. In these cases not the function $L(u)$ is approximated, but that part of it which remains after the elimination of the square root behavior. Namely, we write $L(u) = \sqrt{4g^2 - u^2}\,\hat{L}(u)$, then $\hat{L}(u)$ is approximated by a truncated Chebyshev series and finally the approximate discretized form of the corresponding convolution is very similar to (3.8):

$$\int\limits_0^{2g} dv\, L(v)\, K^S(v, u_{j'}^{(k')}) \simeq \sum_{k=1}^{\mathcal{L}(A_\pm)} \sum_{j=1}^{l_k} \hat{L}_{k,j} \left(\frac{2}{l_k} \sum_{j_0=1}^{l_k} \tilde{C}_{l_k-j+1,j_0} \hat{\mathcal{K}}_{k',j'}^{k,j_0} \right), \qquad (3.10)$$

where $\hat{L}_{k,j} = \hat{L}(v_j^{(k)})$ and $\hat{\mathcal{K}}_{k',j'}^{k,j}$ is the square root factor modified version of (3.9);

$$\hat{\mathcal{K}}_{k',j'}^{k,j} = \int\limits_{A_{\pm,k-1}}^{A_{\pm,k}} dv\, \sqrt{4g^2 - v^2}\, \hat{T}_{j-1}\left(\frac{v - \frac{1}{2}(A_{\pm,k} + A_{\pm,k-1})}{\frac{1}{2}(A_{\pm,k} - A_{\pm,k-1})} \right)\, K^S(v, u_{j'}^{(k')}). \qquad (3.11)$$

Here depending on the left hand side of the equation $u_{j'}^{(k')}$ can stand for $u(t_{j'}^{(k')})$, $t \in [0, B(a)]$ for some a, or it can denote the sampling points on $[0, 2g]$.

Applying our discretization technique to all unknowns and convolutions of our equations, we can reduce the integral equations to a discrete set of nonlinear algebraic equations. However, the transformation from integral equations to algebraic equations is obviously not exact. The typical error comes from the fact that on each subinterval the Chebyshev series is truncated, so the magnitude of the typical errors in our numerical method is governed by the neglected terms of the Chebyshev series, which can be approximated by the magnitude of the last Chebysev coefficient. In our case this is typically somewhere between 10^{-5} and 10^{-6}.

The last step of our numerical method is the iterative solution starting from the asymptotic solution.

---

[14] Such typical combinations are $\log \frac{1 - Y_-}{1 - Y_+}$ and $\log \frac{1 - \frac{1}{Y_-}}{1 - \frac{1}{Y_+}}$.

3.2 The iterative solution

Here we will describe two methods to solve our integral equations iteratively. Since our actual equations have very complicated form, we will describe our methods using a model example, which has similar structure to our equations.

Let the model equations take the form[15]:

$$\log y_a = f_a + G_{ab} \star \log(1 + y_b), \tag{3.12}$$

where G_{ab} are some kernel matrices, f_a are some source terms and y_as are the unknown functions of the problem. The solution of (3.12) is expanded around the asymptotic solution and the equations are formulated in terms of the corrections. To fix the conventions, the correction functions δy_a are defined by:

$$y_a = y_a^o \left(1 + \delta y_a\right). \tag{3.13}$$

As a consequence:

$$\log y_a = \log y_a^o + \log(1 + \delta y_a),$$
$$\log(1 + y_a) = \log(1 + y_a^o) + \log(1 + \mathcal{Y}_a \, \delta y_a), \qquad \mathcal{Y}_a = \frac{y_a^o}{1 + y_a^o}.$$

The source term is also expanded around its asymptotic counterpart: $f_a = f_a^o + \delta f_a$. Then equations (3.12) can be reformulated in terms of the δy_a functions as follows:

$$\log(1 + \delta y_a) = \delta f_a + G_{ab} \star \log(1 + \mathcal{Y}_b \, \delta y_b). \tag{3.14}$$

To define the iterative method, (3.14) are reformulated so that only $O(\delta y_a^2)$ terms remain on the right hand side of the equations. Thus the equations are rewritten in the form:

$$\delta y_a - G_{ab} \star (\mathcal{Y}_b \delta y_b) - \delta f_a = G_{ab} \star [\log(1 + \mathcal{Y}_b \, \delta y_b) - \mathcal{Y}_b \, \delta y_b] - [\log(1 + \delta y_a) - \delta y_a] \,. \tag{3.15}$$

It can be seen that on the left hand side of (3.15) all the quantities are $O(\delta y_a)$, while on the right hand side all the quantities are $O(\delta y_a^2)$. This separation allows us to define an iterative solution. If δy_as are small then the RHS is a small correction

---

[15]For repeated indexes summation is understood.

with respect to the LHS, this is why in an iterative solution the RHS can be simply taken at the value of the previous iteration.

Let $\delta y_a^{(n)}$ the value of δy_a after the nth iteration, then $\delta y_a^{(n+1)}$ can be determined from $\delta y_a^{(n)}$ by solving a set of linear integral equations:

$$\delta y_a^{(n+1)} - G_{ab} \star (\mathcal{Y}_b \delta y_b^{(n+1)}) - \delta f_a = G_{ab} \star \left[\log(1 + \mathcal{Y}_b \, \delta y_b^{(n)}) - \mathcal{Y}_b \, \delta y_b^{(n)} \right] - \left[\log(1 + \delta y_a^{(n)}) - \delta y_a^{(n)} \right].$$
(3.16)

Thus at each step of this iterative method a set of linear integral equations must be solved. Using the discretization method of the previous subsection, the problem reduces to solving a set of linear algebraic equations, which is a straightforward task in numerical mathematics. The very first (0th) iteration starts from the asymptotic solution $\delta y_a = 0$ and it corresponds to the solution of the linearized equations, which in our case gives the Lüscher-formula for the energy.

This (first) method in a certain range of the coupling constant defined a numerically convergent iteration to solve the equations for the ground state of our D-brane anti-D-brane problem, but beyond a certain value of g the method failed to converge anymore. This is why we worked out a second method, which proved to be much more efficient than the first one. This efficiency is manifested in two facts. First it converges much faster than the previous iterative method, second it gives convergent solutions to our equations even when the solution cannot be accepted as physical one[16].

This second method can be described simply in words. Instead of defining an iteration as above, we simply take the discretized version of (3.14). We consider it as a set of nonlinear algebraic equations. As a first step we solve the linearized discrete equations (i.e. (3.16) with RHS = 0) and starting from the solution of the linearized equations we solve the discrete nonlinear system by Newton-method[17].

---

[16]Beyond a certain value of the coupling constant the equations in the form presented in section 2. are not the right ones anymore, they should be corrected by some new source terms and quantization conditions, but even for the "wrong" equations the second method shows numerical convergence, giving unacceptable result.

[17]In MATHEMATICA language it can be implemented by FindRoot[...,Method→"Newton"].

4 Numerical results

In this section we summarize our numerical results. We solved numerically the equations for several integer values of the length parameter L. In this section we concentrate on the states with $L \geq 2$. The $L = 1$ special case is discussed in the next section. For the explanation of the numerical data we will mostly use the $L = 2$ case as an example, because the critical point of this state is the closest one to zero, so it is enough to work with relatively small values of the coupling constant. This is important from the numerical point of view, since by increasing g the numerical method becomes more and more time consuming.

First the parameters of the numerical method is discussed. There are three parameters in the nonlinear integral equations (2.4)-(2.35). The most important one is the coupling constant g, then there are two other parameters which allow us to formulate the equations according to our purposes. The two parameters are p_0 and C, where p_0 is a kind of "truncation index", which tells us the node number starting from which the upper TBA equations are replaced by $SU(4)$ NLIE variables (see figure 1.). The parameter C is a free parameter in the asymptotic solution for the upper $SU(4)$ NLIE variables (C.6-C.20) and it enters the equations such that the asymptotic solution around which the equations are formulated contain this parameter. From this discussion it is obvious that g is a physical parameter which means that the energy depends on it, while the other two parameters p_0 and C correspond to different formulations of the same mathematical problem, so the energy does not depend on them. Thus the choice of these parameters is in our hand and we tried to choose such values for them which allows us numerical convergence in the widest range in g. For example the $C = 0$ choice is the best for numerical purposes since due to (2.22) a $u \to -u$ symmetry arises in the $SU(4)$ HNLIE variables minimizing the number of unknowns in the problem. Tuning p_0 might have two advantages. First, numerical experience shows that for large p_0 the Chebyshev coefficients of the unknowns entering the formula (2.10) for Ω, decay faster, which allows for higher numerical precision. Second also from numerics we learn that with p_0 fixed at certain values of g non physical results are obtained from the numerical solution of the problem. This is a consequence of new local singularities entering the problem, but we still did not take them into account in the equations. These new
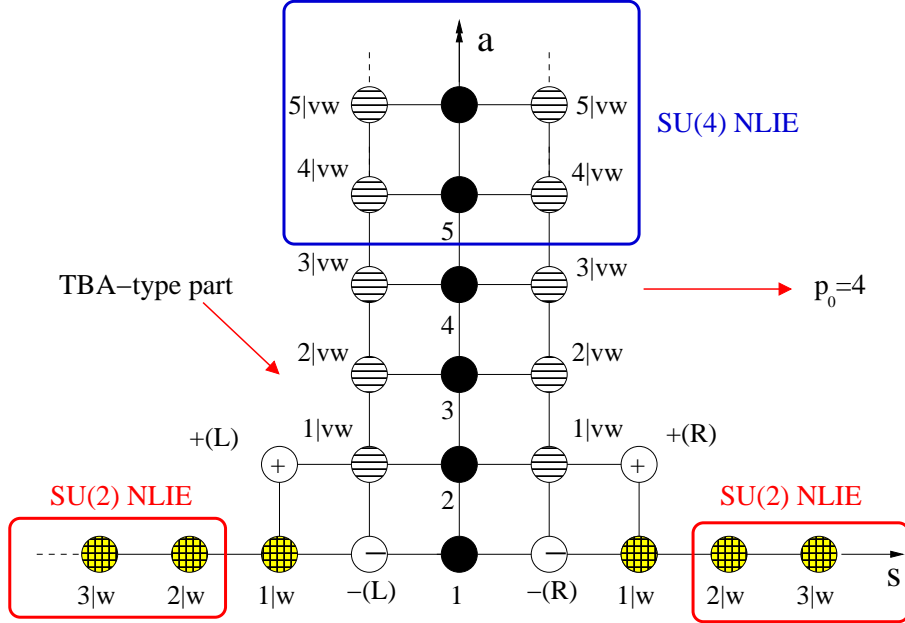
17

Figure 1: The pictorial representation of the Y-system and the HNLIE structure with the choice $p_0 = 4$.

singularities show up mostly in the $SU(4)$ NLIE variables, thus by increasing the value of p_0 the appearance of such singularities in the equations can be postponed to higher values of g.

We solved numerically our equations for different values of L and with various values of p_0 and C, and in case the numerical result was physically acceptable for all p_0 and C we tried, it was also independent of these parameters within the numerical errors of the method.

So far we discussed the parameters of the continuous integral equations and their role in the numerical solution. Now we turn to discuss the numerical parameters of the equations. The numerical parameters are artifacts of the numerical method, and they arise mostly from the discretization method described in section 3. We note that there is no cutoff parameter in our numerical method, neither in the integration range nor in the index of Y-functions. Everything is treated in an exact manner, the only source of numerical errors is the discretization of the unknowns and the convolutions. Here we give the most used subinterval vectors of our numerical computations.

On each subinterval we used an $l_k = 10$ order Chebyshev approximation. The subinterval vector $A_\pm$ of $[0, 2g]$ is given by the empirical formula:

$$A_\pm = \begin{cases} A_{\pm,<} & \text{if } g \leq 2, \\ A_{\pm,>} & \text{if } g \geq 2, \end{cases} \tag{4.1}$$

where the vectors in components take the form:

$$A_{\pm,<}^{(k)} = \frac{2g\,k}{[2g]+1}, \qquad k = 1, ..., [2g] + 1, \tag{4.2}$$

$$A_{\pm,>}^{(k)} = \left\{ \frac{1}{2}, 1, \underline{v}, 2g - \frac{3}{4}, 2g - \frac{1}{2}, 2g - \frac{1}{4}, 2g \right\}, \tag{4.3}$$

with $\underline{v}$ having vector components:

$$v_j = 1 + j\,\frac{2g - 2}{\left[2g - \frac{3}{2}\right]}, \qquad j = 1, ..., \left[2g - \frac{3}{2}\right]. \tag{4.4}$$

Here [...] stands for integer part. The set of subinterval vectors A_Q of $[0, B(Q)]$ could also be given by an appropriate empirical formula, but it would take such a complicated form, that it is better to write down the requirements from which it can be constructed[18]. The requirements can be formulated in the language of the variable $t \in [0, B(Q)]$. The elements of the vector A_Q divide the interval $[0, B(Q)]$ into subintervals. Our requirements constrain the allowed length of the subintervals with respect their location within the whole interval $[0, B(Q)]$. The requirements are as follows:

- The first element of A_Q is $\frac{1}{2}$.

- The length of subintervals Δt in the range $\frac{1}{2} < t < 2$ is approximately $\frac{1}{3}$: $\Delta t \lessapprox \frac{1}{3}$.

- The length of subintervals in the range $2 < t < 3$ is approximately $\frac{1}{2}$: $\Delta t \lessapprox \frac{1}{2}$.

- The length of subintervals in the range $3 < t < B(Q)$ is approximately 1: $\Delta t \lessapprox 1$.

---

[18]These requirements are based on numerical experiences with the choice $l_k \geq 10$.

In practice the length of the subintervals are slightly "squeezed" with respect to the conditions above to fill the full $[0, B(Q)]$ properly[19].

Finally, we note that for checking the numerical precision, we also did numerical computations with $l_k = 12, 14, 16$ keeping the subintervals fixed and also with keeping $l_k = 10$, but doubling the number of subinterval points.

Before turning to present the numerical results we would like to say a few words about the possible tests of the numerical results. Namely, how one can recognize a wrong result. This is also a very important point of the numerical method, since there are a lot of equations with very complicated kernels and it is easy to make mistakes during writing the code of the numerical solution. There are three basic things that we can check from the numerical results.

The first check is dictated by the energy equation (2.12). It is known that the energy starts at the first wrapping order (i.e. e^{-L}) and this first order correction is exactly given by the Lüscher formula [4]:

$$\Delta E(L) = -\sum_{Q=1}^{\infty} \int_0^{\infty} \frac{du}{2\pi} \frac{d\tilde{p}_Q}{du} Y_Q^o(u), \qquad (4.5)$$

with $Y_Q^o(u)$ given explicitly in (D.2). This quantity can be computed numerically with any digits of precision, so its value is known exactly at any values of g and L. The Lüscher-formula (4.5) corresponds to the linearized version of our equations (2.4)-(2.35), this is why solving the linearized set of equations (which is the first step for the iterative solution) we should reproduce the numerical evaluation of (4.5). This is a nontrivial check on the kernels, on the discretization method and on the equations themselves as well. In addition since this test is quantitative it can tell some information also on the numerical precision of the method[20].

This test can signal problems on solving the linearized problem. The remaining two tests can signal some discrepancies during the solution of the nonlinear problem.

The second testing condition is that from the numerical solution $Y_{p_0-2|vw}$ must be real. This sound trivial, but it is not trivial at all. If one takes a look at the equation

---

[19]Not to have very small subintervals: $\Delta t \lesssim 0.1$.

[20]If one experiences that the numerical solution of the linearized problem agrees with the numerical value of (4.5) within certain digits of precision, than the deviation from the Lüscher result can be a good starting estimate to the numerical error. One cannot expect better accuracy, but the precision will not become much worse either.

(2.32) of $Y_{p_0-2|vw}$, one can recognize that there are complex quantities on the RHS which do not form conjugate pairs. So, the reality of the LHS is not guaranteed by the form of the equations, but it is guaranteed by the form of the solution. Thus the second testing condition is expressed by the inequality:

$$|\text{Im} \log Y_{p_0-2|vw}| \leq \text{Numerical error}, \qquad 10^{-6} \gtrsim \text{Numerical error} \gtrsim 10^{-9}. \quad (4.6)$$

Here we wrote the typical numerical errors we had during the computations.

The third test is based on the approximation scheme we use. One must check whether the Chebyshev coefficients of the unknowns decay as it is expected. From such a check the numerical precision of the method can be read off and it can shed light on some anomalous divergent behavior of the numerical solution. Thus it can indicate possible errors in the elimination of the divergent $\ln u$ terms in (2.2) and (2.36,2.37).

The numerical results for the $L = 2$ case can be seen in figure 2 and table 1. In the table we show not only the energy E_{BTBA} at different values of the coupling g, but the constant δc, as well. The other columns of the table are related to the solution of the linearized equations; $E_{BTBA}^{(0)}$ and $\delta c^{(0)}$ are the energy and the global constant from the numerical solution of the linearized equations. $\Delta E_{BTBA}^{(0)}$ stands for the deviation of $E_{BTBA}^{(0)}$ from the exact Lüscher result. This quantity gives some information on the numerical accuracy of the method. Finally the column "number of nodes" tells us the cutoff index of the Lüscher formula, which is necessary to get the Lüscher energy with the precision given by $\Delta E_{BTBA}^{(0)}$. This number is not equal to p_0 in our equations. For the $L = 2$ state, in case of $0 < g < 1.9$ we used $p_0 = 4$, for $1.9 < g < 2.1$ we used $p_0 = 8$, and in the range $2.1 < g < 2.14$ we took $p_0 = 12$. Finally at $g = 2.16$ we used $p_0 = 26$ to get acceptable numerical results. Then beyond this point we could not save our equations from the entrance of new singularities by increasing the value of p_0 with a reasonable $O(10)$ amount. Because of this reason we could not get really close to the supposed critical point. There $E_{BTBA} \sim -1$, but we could reach only $E_{BTBA} \sim -0.7$ at $g = 2.16$. Apart from this very embarrassing fact, some important features can be read off from the numerical data. First of all it can be seen that in the range $g < 2.16$ the energy is very slowly varying function of g, so there is no sign of any divergent behavior. What is more interesting is the behavior of the global constant δc. It is negative and it decreases

21

faster and faster as g is increased. From the definition of δc (2.2) it follows that all Y_Q-functions are proportional to its exponent: $Y_Q \sim \xi = e^{\delta c}$. The fast decrease of δc indicates that though Y_Q has worse and worse large u asymptotic by the increase of g, its global magnitude is actually decreasing. This remark can be understood from the TBA formulation of the energy.

$$E_{BTBA} = -\sum_{Q=1}^{\infty} \int_{0}^{\infty} \frac{du}{2\pi} \frac{d\tilde{p}_Q}{du} \log(1 + Y_Q(u)). \qquad (4.7)$$

Close to the critical point E_{BTBA} is supposed to be finite [4] $E_{BTBA} \sim 1 - L$, but naively the sum in the RHS of (4.7) would diverge due to the large Q terms. Since Y_Q is small for large Q, in leading order[21] the $\log(1 + Y_Q) \to Y_Q$ replacement can be done:

$$E_{BTBA} = \underbrace{-\sum_{Q=1}^{Q_0} \int_{0}^{\infty} \frac{du}{2\pi} \frac{d\tilde{p}_Q}{du} \log(1 + Y_Q(u))}_{\text{Finite}} - \xi \underbrace{\sum_{Q=Q_0}^{\infty} \int_{0}^{\infty} \frac{du}{2\pi} \frac{d\tilde{p}_Q}{du} \tilde{Y}_Q(u)}_{\text{Diverges close to the critical point}} + ..., \quad (4.8)$$

where Q_0 is an arbitrary index cutoff scale and $Y_Q = \xi \tilde{Y}_Q$ replacement was applied. Since ξ is Q-independent all the dangerous Q dependence is still in $\tilde{Y}_Q$. In (4.8) approaching to the critical point the second sum starts to diverge, and the global multiplicative factor ξ must tend to zero in order to ensure the finiteness of both sides of the equation. Our numerical data seems to support this picture. Namely $\delta c \to -\infty$ as going closer and closer to the critical point.

In [4] from Y-system arguments the large Q behavior of Y_Q was also estimated by the formula:

$$Y_Q(u) \simeq \xi(g) \frac{1}{\left(u^2 + \frac{Q^2}{g^2}\right)^{2E_{BTBA}}} Y_Q^o(u), \qquad \xi = e^{\delta c}, \qquad (4.9)$$

where δc is defined after (2.2) in section 2. (4.9) is a very important formula, because it plays crucial role in the analytical determination of the critical point. Since the numerical solution of the HNLIE equations of section 2. does not require the introduction of any index cutoff, it takes into account the contributions of all
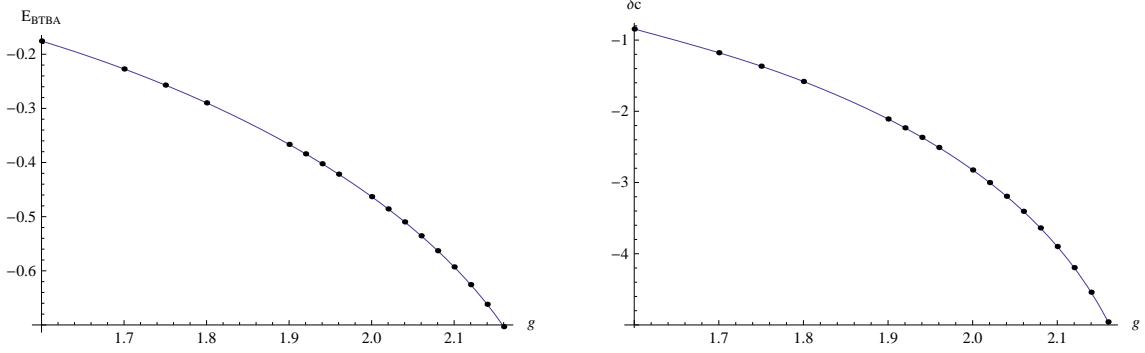
---

[21]For large Q.

Figure 2: E_{BTBA} (on the left) and δc (on the right) as functions of g for the $L = 2$ state.

g	E_{BTBA}	δc	$E_{BTBA}^{(0)}$	$\delta c^{(0)}$	$\Delta E_{BTBA}^{(0)}$	number of nodes
1.6	-0.175553	-0.844383	-0.185898	-0.893355	$3.7 \cdot 10^{-6}$	25
1.7	-0.2271599	-1.17751	-0.24183601	-1.21357	$4.9 \cdot 10^{-6}$	25
1.75	-0.25693719	-1.36622	-0.2738668	-1.40256	$5.7 \cdot 10^{-6}$	27
1.80	-0.2897776	-1.58077	-0.3088130	-1.61278	$6.3 \cdot 10^{-6}$	28
1.90	-0.366494169	-2.10766	-0.38810198	-2.10321	$7.9 \cdot 10^{-6}$	30
1.92	-0.38393979	-2.23237	-0.40555472	-2.21339	$8.2 \cdot 10^{-6}$	30
1.94	-0.402255118	-2.36573	-0.4235649	-2.32785	$8.7 \cdot 10^{-6}$	30
1.96	-0.42147149	-2.50781	-0.4421440	-2.44671	$9.0 \cdot 10^{-6}$	30
2.00	-0.46303978	-2.82377	-0.4810544	-2.69809	$9.9 \cdot 10^{-6}$	31
2.02	-0.48564199	-3.00085	-0.5014098	-2.83086	$9.9 \cdot 10^{-6}$	32
2.04	-0.50966430	-3.19333	-0.52237993	-2.96847	$1.0 \cdot 10^{-5}$	32
2.06	-0.53532776	-3.40422	-0.5439774	-3.11107	$1.0 \cdot 10^{-5}$	32
2.08	-0.56291307	-3.63744	-0.566214	-3.25878	$1.0 \cdot 10^{-5}$	33
2.10	-0.592805	-3.89861	-0.589106	-3.41179	$8.9 \cdot 10^{-6}$	35
2.12	-0.625515	-4.19506	-0.612655	-3.56999	$1.2 \cdot 10^{-5}$	34
2.14	-0.661868	-4.54055	-0.636888	-3.73339	$9.6 \cdot 10^{-6}$	36
2.16	-0.7031687	-4.956683	-0.661809	-3.90338	$7.0 \cdot 10^{-6}$	39

Table 1: Numerical data for the $L = 2$ state.

23

the Y-functions of the infinite Y-system. This makes it possible to test numerically the correctness of the large Q estimate (4.9). In case (4.9) holds, it implies that $\delta \ln \bar{y}_Q = \ln \bar{y}_Q - \ln \bar{y}_Q^o$ tends to zero as $1/Q$ for large Q. In figure 3. the numerical demonstration of this statement can be seen. The plotted functions are defined by the formula:

$$\delta \mathcal{F}_Q(t) = \begin{cases} \delta \ln \bar{y}_Q \left(x_Q(B(Q) - t) \right) & \text{if} \quad t > 0, \\ \delta \ln \bar{y}_Q \left(-x_Q(B(Q) + t) \right) & \text{if} \quad t < 0, \end{cases} \qquad (4.10)$$

where $x_Q(t) = Q \left(\frac{B(Q)}{t} - 1 \right)$, $B(Q) = \frac{2g}{Q} + 1$. The plots of figure 3. are based on the numerical computation with $p_0 = 26$ at $g = 2.16$. Figure 3. nicely demonstrates the expected $1/Q$ behavior of the functions $\delta \mathcal{F}_Q$.
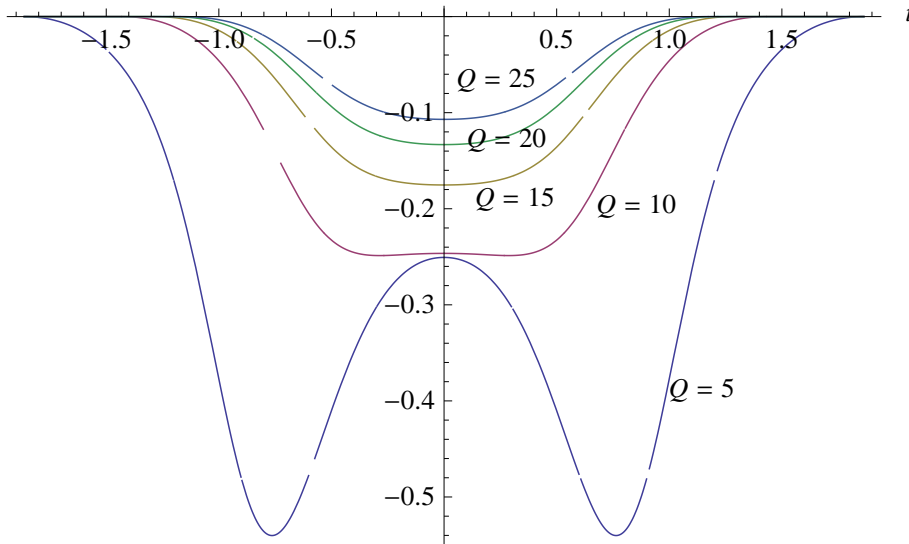

Figure 3: Large Q behavior of $\delta \mathcal{F}_Q$ from numerical data at $g = 2.16$ with $p_0 = 26$.

For the $L = 2$ state beyond $g = 2.16$ the numerical solution of the discretized problem did not give physically acceptable results. To get some insight into the source of the problems, at $g = 2.18$ we plotted the imaginary part of the LHS of the last equation in (2.18), namely $\text{Im} \log(1 + \delta b_6)$ at $u = x_{p_0}(B(p_0) - t)$. Figure 4. shows that there is a jump of 2π, when t is close to $B(p_0)$. (I.e. large u.)[22]

---

[22]Here the sampling points are connected according to the Chebyshev approximation. This is why the jump of the logarithm is not "sharp".

24

This fact shows us that the equations we solved numerically are not the right ones anymore. Something is missing from the equations. Either a special object [44, 45] or some other local singularities of the T- and Q-functions of the problem, which enter those strips of the complex plane, which are relevant in the derivation of the HNLIE equations.

The numerical data for the $L = 3$ and $L = 4$ states are given by table 2 and 3. Also in case of these states the appearance of new singularities obstacled us to get close to the critical point in the framework of the HNLIE technique.
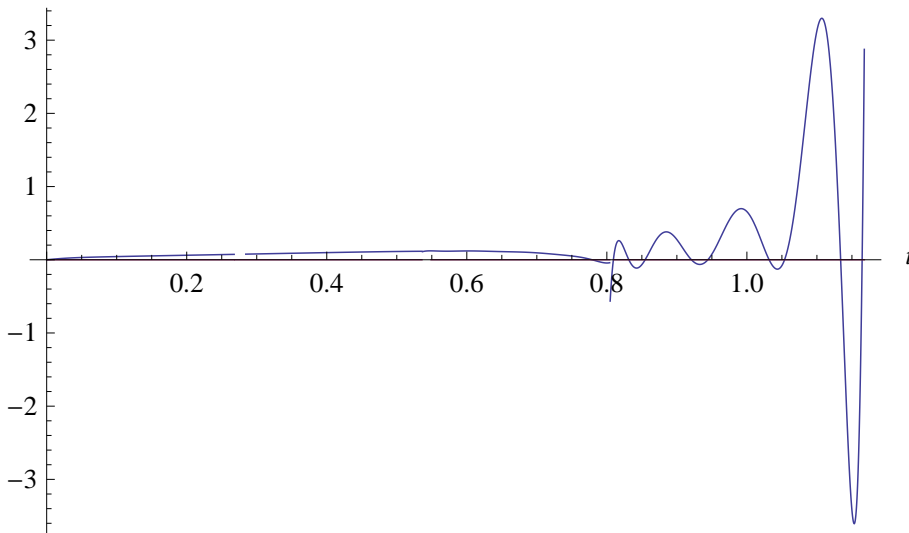

Figure 4: The anomalous behavior of $\mathrm{Im}\log(1 + \delta b_6)$ at $g = 2.18$ and $p_0 = 26$.

5 Comments on the $L = 1$ case

The $L = 1$ ground state is mysterious, since so far the anomalous dimension of this state could not be determined even for small g either from field theory or from integrability considerations [4]. Here we concentrate on the integrability side. There the boundary Lüscher formula [27, 39] diverges for this state [4]. For generic L the Lüscher formula is simply the expansion of the TBA energy formula around the asymptotic solution with the replacement: $\log(1 + Y_Q) \to Y_Q^o$. For small coupling it

g	E_{BTBA}	δc	$E_{BTBA}^{(0)}$	$\delta c^{(0)}$	$\Delta E_{BTBA}^{(0)}$
2.2	-0.114591	-0.62945	-0.12907	-0.711869	$8.4 \cdot 10^{-7}$
2.6	-0.21909	-1.33443	-0.267823	-1.641000	$3.0 \cdot 10^{-7}$
2.8	-0.286833	-1.82583	-0.366547	-2.34855	$2.1 \cdot 10^{-6}$
3.0	-0.365866	-2.42503	-0.488968	-3.26271	$2.9 \cdot 10^{-6}$
3.2	-0.457294	-3.14677	-0.638504	-4.42131	$8.7 \cdot 10^{-6}$
3.4	-0.56282	-4.01232	-0.818842	-5.86636	$1.1 \cdot 10^{-5}$
3.6	-0.685108	-5.05271	-1.03391	-7.64329	$1.5 \cdot 10^{-5}$

Table 2: Numerical data for the $L = 3$ state.

g	E_{BTBA}	δc	$E_{BTBA}^{(0)}$	$\delta c^{(0)}$	$\Delta E_{BTBA}^{(0)}$
2.6	-0.0716174	-0.427755	-0.0793412	-0.476413	$6.0 \cdot 10^{-7}$
2.8	-0.0975242	-0.607523	-0.111564	-0.699788	$1.1 \cdot 10^{-8}$
3.0	-0.128116	-0.829046	-0.151888	-0.991352	$4.2 \cdot 10^{-8}$
3.2	-0.163439	-1.0949	-0.201422	-1.36341	$9.2 \cdot 10^{-8}$
3.4	-0.203514	-1.40733	-0.261362	-1.82949	$9.8 \cdot 10^{-8}$
3.6	-0.24835	-1.76832	-0.332987	-2.40437	$7.0 \cdot 10^{-7}$
4.0	-0.35239	-2.64384	-0.51686	-3.94631	$8.6 \cdot 10^{-7}$
4.2	-0.411691	-3.16247	-0.632106	-4.9496	$2.7 \cdot 10^{-6}$
4.4	-0.545354	-4.3733	-0.917326	-7.52081	$1.3 \cdot 10^{-6}$

Table 3: Numerical data for the $L = 4$ state.

takes the form [4]:

$$\Delta E(L) = -\sum_{Q=1}^{\infty} \int_0^{\infty} \frac{du}{2\pi} \frac{d\tilde{p}_Q}{du} Y_Q^o(u) \simeq -\left(\frac{g}{2}\right)^{4L} \left\{ \frac{4}{4L-1} \binom{4L}{2L} \zeta(4L-3) + O(g^2) \right\}.$$
(5.1)

This small coupling expression diverges for $L = 1$, since this point sits exactly on the pole of the ζ-function. As for the origin of this divergence; in (5.1) the individual integrals are convergent, but their sum for Q causes the divergence. In [4] it was argued that also for any larger L the TBA energy formula would diverge beyond a certain critical value of the coupling: $g_c(L)$. Assuming that the energy is a monotonously decreasing function of g, which is supported by numerical results, this critical point can be expressed clearly in terms of the energy by the criterion:

$$E_c(L) \equiv E(g_c(L)) = 1 - L.$$
(5.2)

In [4] this point was interpreted as a turning point where the energy becomes imaginary and as a physical consequence the ground state becomes tachyonic. For the $L = 1$ state the critical point is right at $g = 0$ assuming that for small g the energy is also small.

Now let us turn our attention to the HNLIE description of the problem detailed in section 2. Here there are no infinite sums and even for $L = 1$ all the convolutions of the integral equations seem to converge[23]. For the first sight there is no sign of any problem in the HNLIE description and it seems that only the TBA description is inappropriate to treat the $L = 1$ case. But unfortunately this is not the case.

We can write down the discretized integral equations for the $L = 1$ case as well, and using the Newton-method, we can solve them for small values of the coupling[24]. We always get some numerical solution for the discretized problem, but it turns out that the Chebyshev coefficients of the unknowns, which correspond to the large u subinterval do not form a decaying series. This phenomenon is a typical sign of some weak (probably logarithmic) large u divergence of the unknowns. If one increases the number of subintervals and sampling points the situation remains the same. The

---

[23]If we assume that large u behavior of the unknown functions, which was used to derive the BTBA equations from discontinuity relations and Y-system.

[24]Typically $g \sim 10^{-1}$.

conclusion is that we can solve the discretized problem, but the solution cannot be interpreted as the discretely approximated version of the continuous solution of our integral equations. In other words the continuous HNLIE equations have no solution for $L = 1$.

In order to get some analytical insight why the solutions become diverging at large u let us consider the TBA formulation of the problem ($p_0 \to \infty$ in HNLIE). It is known [4] that the TBA energy comes from the coefficient of the most divergent $\log|u|$ term in the large u expansion of $\log Y_Q$:

$$\log Y_Q(u) = -4(L + E_{BTBA}) \log|u| + O(1). \tag{5.3}$$

The E_{BTBA} term originates from the RHS of the TBA equations for $\log Y_Q$ from the convolution term $\sum_{Q'=1}^{\infty} \log(1 + Y_{Q'}) \star K_{\mathfrak{sl}(2)}^{Q'Q}$ by exploiting the large u expansion of the kernel: $K_{\mathfrak{sl}(2)}^{Q'Q}(v, u) = -\frac{1}{\pi} \frac{d\tilde{p}_{Q'}}{dv} \log|u| + O(1)$. $K_{\mathfrak{sl}(2)}^{Q'Q}$ has better large Q' behavior than that of $\frac{d\tilde{p}_{Q'}}{dv}$, since it behaves like $1/Q'$. As a consequence contrary to the energy formula, the sum of dressing convolutions is convergent indeed. Thus one might think that for $L = 1$ the problem emerges, because for the derivation of the energy formula we expanded the sum of dressing convolutions term by term for large u. This is why instead of this usual procedure, we consider the sum of dressing convolutions itself, compute it and then at the end of the computation we take the large u expansion. This procedure is carried out in the small coupling limit. We need the leading order small coupling expression of the dressing kernel in the mirror-mirror channel[25]:

$$K_{\mathfrak{sl}(2)}^{Q'Q,(0)}(u_1, u_2) = -\frac{1}{2\pi} \left[\psi\left(1 + \frac{Q'}{2} - i\frac{i}{2}u_1\right) + \psi\left(1 + \frac{Q'}{2} + i\frac{i}{2}u_1\right) \right.$$
$$\left. - \psi\left(1 + \frac{Q'+Q}{2} + i\frac{i}{2}(u_2 - u_1)\right) - \psi\left(1 + \frac{Q'+Q}{2} - i\frac{i}{2}(u_2 - u_1)\right) \right] + \dots \tag{5.4}$$

Then the formula, the large u expansion of which accounts for the small coupling expanded energy, is given by:

$$\mathcal{O}(u, Q) = \sum_{Q'=1}^{\infty} \int_{-\infty}^{\infty} \frac{dv}{4\pi} Y_{Q'}^{o,(L=1)}(v) \, K_{\mathfrak{sl}(2)}^{Q'Q,(0)}(v, u), \tag{5.5}$$

---

[25]Here we use the rapidity convention where the branch points are at $\pm 2g$.

where $Y_Q^{o,(L=1)}(u) = g^4 \frac{16\,Q^2\,u^2}{(u^2+Q^2)^3}$ is the leading small coupling expression of (D.2) at $L = 1$. The second derivative of $\mathcal{O}(u,Q)$ can be computed explicitly by simple Fourier space technique. We take the Fourier form of each functions under integration, the convolution is the product of the individual Fourier transforms, the sum for Q' can be easily done in Fourier space and at the end of the process everything is transformed back to the u space. In such a manner one gets a bulky, but explicit expression for $\frac{d^2}{du^2}\mathcal{O}(u,Q)$, which we do not present here, only its large u expansion:

$$\frac{d^2}{du^2}\mathcal{O}(u,Q) = 4\,g^4 \left(\frac{3}{2} - \gamma_E + 2\ln 2\right)\frac{1}{u^2} - 8\,g^4 \frac{\log u}{u^2} + O(\frac{1}{u^3}). \qquad (5.6)$$

Integrating twice the large u expansion at small coupling becomes:

$$\mathcal{O}(u,Q) = 4\,g^4 \left(\frac{1}{2} + 2\,\gamma_E - \ln 4\right)\log u + 4\,g^4\,(\log u)^2 + ... \qquad (5.7)$$

From (5.7) it is obvious why the naive Lüscher energy formula diverged. Because the leading order large u term is not the expected $\sim \log|u|$, but $\sim (\log u)^2$. This is the key point of the problem, since in this case after this first iteration Y_Q acquires an unwanted type of large u term, which makes Y_Q divergent for large u:

$$Y_Q(u) \sim u^{\left(-4L+4\,g^4\left(\frac{1}{2}+2\,\gamma_E-\ln 4\right)+...\right)}\,e^{4\,g^4\,(\log u)^2+...}. \qquad (5.8)$$

This large u divergence contradicts to what was assumed about the large u behavior of Y_Q at the derivation of the integral equations, since it was supposed to decay. In this example we have shown in the small coupling limit, that during the iterative solution of the BTBA equations, $\log Y_Q$ acquires an extra $\sim (\log|u|)^2$ behavior at infinity, which made Y_Q an exploding function at infinity. This means that the iterative solution of the TBA equations leaves the class of physically acceptable solutions.

One might ask the question, whether it is possible to keep somehow the qualitative large u behaviors that we assumed at the derivation of the equations? Here we sketch a possible idea for small coupling to the $L = 1$ case.

Let us assume that we managed to modify the TBA equations, such that all Y-functions have the large u behavior we want. Since most of the TBA equations reflect the structure of the Y-system functional equations we expect to modify only those equations which are affected by also the discontinuity relations. It follows,

that for large Q, the formula for the estimate for Y_Q (4.9) remains the same. Now, we assume that for small g the energy is also small and take the simultaneous small g and small energy expansion of the RHS of the TBA energy formula (4.7). In leading order the large Q terms will dominate:

$$
\begin{aligned}
E_{BTBA} &\simeq -\sum_{Q=1}^{\infty} \int_{-\infty}^{\infty} \frac{du}{4\pi} \hat{Y}_Q\left(\frac{u}{g}\right) = -\tilde{\xi} \sum_{Q=1}^{\infty} \int_{-\infty}^{\infty} \frac{du}{4\pi} \left(g^2\right)^{2L} 16Q^2 \frac{u^2}{(u^2+Q^2)^{2(L+E_{BTBA})+1}} \\
&= -\frac{\tilde{\xi}}{2^{4(L+E_{BTBA})}} \frac{4g^{4L}}{4(L+E_{BTBA})-1} \binom{4(L+E_{BTBA})}{2(L+E_{BTBA})} \sum_{Q=1}^{\infty} \frac{1}{Q^{(4(L+E_{BTBA})-3)}} \\
&= -\frac{\tilde{\xi}}{2^{4(L+E_{BTBA})}} \frac{4g^{4L}}{4(L+E_{BTBA})-1} \binom{4(L+E_{BTBA})}{2(L+E_{BTBA})} \zeta(4(L+E_{BTBA})-3) \\
&\simeq -\frac{\tilde{\xi}\, g^4}{8\, E_{BTBA}} + O(\tilde{\xi} g^4),
\end{aligned}
$$

(5.9)

where $\hat{Y}_Q$ denotes the large Q estimate (4.9) of Y_Q, $\tilde{\xi} = \xi\, g^{4E_{BTBA}}$ as a consequence of the $u \to u/g$ change of variables and the pole term in E_{BTBA} comes from the pole of the ζ-function. In our HNLIE approach the energy E_{BTBA} and the constant δc are parts of the equations which means that they are not simply expressed by explicit formulas based on the solution of the equations, but must me obtained by solving the set of non-trivially entangled equations. In this sense (5.9) defines an equation for E_{BTBA} for small g. Its leading order solution is:

$$
E_{BTBA} = g^2 \sqrt{-\tilde{\xi}} + \dots. \tag{5.10}
$$

If $\tilde{\xi} > 0$ then E_{BTBA} becomes imaginary as it would be expected from string-theory expectations [4]. To decide the sign of $\tilde{\xi}$, the equation (2.13) has to be analyzed in the context of the small g and E_{BTBA} expansion. It turns out that $\tilde{\xi}$ is positive and $O(1)$ for small g, so according to (5.10) E_{BTBA} is imaginary. Another remarkable fact is that according to (5.10) E_{BTBA} starts at $O(g^2)$ instead of the $O(g^4)$ prediction of the boundary Lüscher formula (5.1). This might be another explanation why the coefficient of g^4 diverges in the Lüscher formula for the $L = 1$ case. Finally, we note that in the small g and E_{BTBA} expansion of the $L = 1$ state, the energy is pure imaginary only at leading order in g, but in higher orders it acquires real part as well.

30

For the first sight, it might seem that without modifying the equations one immediately gets imaginary energy when going through the critical point. But, the situation is a bit more subtle. There is a hidden tacit modification of the equations. This is realized in (5.9) by the replacement:

$$\sum_{Q=1}^{\infty} \frac{1}{Q^{4(L+E_{BTBA})-3}} \to \zeta(4(L+E_{BTBA})-3).$$

For the $L=1$ case it is an identity for $\text{Re}(E_{BTBA}) > 0$, but for $\text{Re}(E_{BTBA}) < 0$ it is not an identity anymore, but a nontrivial analytical continuation in E_{BTBA}.

Such an analytical continuation would require the exact determination of complicated sums of convolutions of the TBA equations as functions of the energy. Since this does not seem to be feasible in practice, we give such an alternative modification of the TBA equations which preserves the infinite sum structure of the equations, but the sums will converge everywhere for $\text{Re}(E_{BTBA}) > -L$ except at the critical value $E_{cr} = 1 - L$.

The basic idea of the modification comes from the sum representations of the ζ-function. The usual one converges for $\text{Re}(s) > 1$:

$$\zeta(s) = \sum_{Q=1}^{\infty} \frac{1}{Q^s}, \qquad \text{Re}(s) > 1, \tag{5.11}$$

but there is another representation which converges for $\text{Re}(s) > 0$:

$$\zeta(s) = \frac{1}{s-1} \sum_{Q=1}^{\infty} \left(\frac{Q}{(Q+1)^s} - \frac{Q-s}{Q^s} \right), \qquad \text{Re}(s) > 0. \tag{5.12}$$

Then the original TBA equations are modified through their infinite sums by the replacements:

$$\sum_{Q=1}^{\infty} L_Q \star \mathcal{K}_Q \to \frac{1}{s_E - 1} \sum_{Q=1}^{\infty} \left\{ Q \cdot (L_{Q+1} \star \mathcal{K}_{Q+1}) - (Q - s_E) \cdot (L_Q \star \mathcal{K}_Q) \right\}, \tag{5.13}$$

where $s_E = 4(L + E_{BTBA}) - 3$. Taking into account the large Q behavior of all Y_Q functions and all the kernels of the infinite sums of the TBA equations, the new representation will converge for $\text{Re}(E_{BTBA}) > -L$. This slight modification of the TBA equations might make it possible to go beyond the critical point and get

solution of the TBA equations with large u asymptotics being in accordance with the ones used for the derivation of the equations.

The conclusion of this heuristic argument is that to keep the expected[26] qualitative large u behavior a nontrivial modification of the TBA equations must be carried out, which might lead to complex energies.

6   Summary and conclusions

In this paper we studied the ground state energy of a pair of open strings stretching between a coincident $D3$-brane anti-$D3$-brane pair in S^5 of $AdS_5 \times S^5$. The main motivation for the study is that string-theory predicts that the ground state of such a configuration becomes tachyonic for large values of the 't Hooft coupling [4].

In [4] it was shown that the usual integrability based BTBA approach always give real energies for the ground state and it breaks down at latest when the energy gets close to the critical value: $E_c(L) = 1 - L$. This point was interpreted in [4] as a transition point where the ground state becomes tachyonic.

Approaching this critical point the contribution of all the Y-functions of the BTBA becomes quantitatively relevant, thus the numerical solution of the truncated BTBA equations cannot give accurate results close to the critical point. To resolve this difficulty and get more accurate numerical results we transformed the previously proposed BTBA equations into finite component HNLIE equations. The HNLIE equations were solved at different values of g and L and the numerical results confirmed the earlier BTBA data.

During the numerical solution of the HNLIE equations the usual iterative methods failed to converge, this is why we worked out two numerical methods to reach convergence. The most effective one is, if one transforms the integral equations into discrete nonlinear algebraic equations and solves them by Newton-method. The power of this method is demonstrated by the fact that it gives convergent results even if the numerical solution is not physically acceptable.

Unfortunately, in our numerical studies we could not get very close to the critical point, because new singularities entered the HNLIE equations taking into account of

---

[26]This primarily means that $\log Y_Q \sim \log |u|$ for large u, while other Y-functions tend to constant.

which would have required an enormous amount of additional work. Nevertheless, in the range where we could get physically acceptable results, the precision of the HNLIE data were higher than those of BTBA and the HNLIE approach could give a deeper understanding of the problem.

For the ground state of the $L = 1$ state the critical point is right at $g = 0$ and neither perturbative field theory computations nor the boundary Lüscher formula could provide a finite quantitative answer to the anomalous dimension. Even in this special case the numerical solution of the HNLIE equations was possible. The results showed that without an appropriate modification of the equations, they cannot give physically acceptable results. In this case, it means that the solution of the dicretized problem cannot be considered as a discretized solution of the continuous nonlinear integral equations. Moreover the large rapidity behavior of the numerical solution is incompatible with the one assumed for the derivation of the equations. This phenomenon is analytically analyzed in the framework of BTBA and an idea is sketched to preserve the expected large rapidity behavior of the unknowns. This method is based on an appropriate modification of the TBA equations which would lead to complex energies beyond the critical point.

Hopefully the $L = 1$ case at $g = 0$ could be treated analytically in the framework of the quantum spectral curve method [47, 48, 14], solving the mystery of this state in the context of integrability.

A Notations, kinematical variables, kernels

Throughout the paper we use the basic notations and TBA kernels of ref. [41], which we summarize below. For any function f, we denote $f^{\pm}(u) = f(u \pm \frac{i}{g})$ and in general $f^{[\pm a]}(u) = f(u \pm \frac{i}{g}a)$, where the relation between g and the 't Hooft coupling λ is given by $\lambda = 4\pi^2 g^2$. Most of the kernels and also the asymptotic solutions of the HNLIE-system are expressed in terms of the function $x(u)$:

$$x(u) = \frac{1}{2}(u - i\sqrt{4 - u^2}), \qquad \operatorname{Im} x(u) < 0, \qquad (A.1)$$

which maps the u-plane with cuts $[-\infty, -2] \cup [2, \infty]$ onto the physical region of the mirror theory, and in terms of the function $x_s(u)$

$$x_s(u) = \frac{u}{2}\left(1 + \sqrt{1 - \frac{4}{u^2}}\right), \qquad |x_s(u)| \geq 1, \qquad (A.2)$$

which maps the u-plane with the cut $[-2, 2]$ onto the physical region of the string theory. Both functions satisfy the identity $x(u) + \frac{1}{x(u)} = u$ and they are related by the $x(u) = x_s(u)$, and $x(u) = 1/x_s(u)$ relations on the lower and upper half planes of the complex plane respectively.

The momentum $\tilde{p}^Q$ and the energy $\tilde{\mathcal{E}}_Q$ of a mirror Q-particle are expressed in terms of $x(u)$ as follows:

$$\tilde{p}_Q(u) = gx\left(u - \frac{i}{g}Q\right) - gx\left(u + \frac{i}{g}Q\right) + iQ, \qquad \tilde{\mathcal{E}}_Q(u) = \log\frac{x\left(u - \frac{i}{g}Q\right)}{x\left(u + \frac{i}{g}Q\right)}. \qquad (A.3)$$

Two different types of convolutions appear in the HNLIE equations. These are:

$$f \star \mathcal{K}(v) \equiv \int_{-\infty}^{\infty} du\, f(u)\, \mathcal{K}(u, v), \quad f \,\hat{\star}\, \mathcal{K}(v) \equiv \int_{-2}^{2} du\, f(u)\, \mathcal{K}(u, v).$$

The kernels and kernel vectors entering the HNLIE equations can be grouped into two sets. The kernels from the first group are functions of only the difference of the rapidities, thus actually they depend on a single variable. The other group of kernels composed of those, which are not of difference type.

We start with listing the kernels depending on a single variable:

$$s(u) = \frac{1}{2\pi i}\frac{d}{du}\log\tau^-(u) = \frac{g}{4\cosh\frac{\pi gu}{2}}\,, \quad \tau(u) = \tanh[\frac{\pi g}{4}u]\,,$$

$$K_Q(u) = \frac{1}{2\pi i}\frac{d}{du}\log S_Q(u) = \frac{1}{\pi}\frac{g\,Q}{Q^2 + g^2 u^2}\,, \quad S_Q(u) = \frac{u - \frac{iQ}{g}}{u + \frac{iQ}{g}}\,,$$

$$K_{MN}(u) = \frac{1}{2\pi i}\frac{d}{du}\log S_{MN}(u) = K_{M+N}(u) + K_{N-M}(u) + 2\sum_{j=1}^{M-1} K_{N-M+2j}(u)\,,$$

$$S_{MN}(u) = S_{M+N}(u)S_{N-M}(u)\prod_{j=1}^{M-1} S_{N-M+2j}(u)^2 = S_{NM}(u)\,. \tag{A.4}$$

The fundamental building block of kernels which are not of difference type is:

$$K(u,v) = \frac{1}{2\pi i}\frac{d}{du}\log S(u,v) = \frac{1}{2\pi i}\frac{\sqrt{4-v^2}}{\sqrt{4-u^2}}\frac{1}{u-v}\,, \quad S(u,v) = \frac{x(u) - x(v)}{x(u)x(v) - 1}\,. \tag{A.5}$$

Using the kernels $K(u,v)$ and $K_Q(u-v)$ it is possible to define a series of kernels which are connected to the fermionic $Y_\pm$-functions. They are:

$$K_{Qy}(u,v) = K(u - \frac{i}{g}Q, v) - K(u + \frac{i}{g}Q, v)\,, \tag{A.6}$$

$$K_{\mp}^{Qy}(u,v) = \frac{1}{2}\Big(K_Q(u-v) \pm K_{Qy}(u,v)\Big) \tag{A.7}$$

and

$$K_{yQ}(u,v) = K(u, v + \frac{i}{g}Q) - K(u, v - \frac{i}{g}Q)\,, \tag{A.8}$$

$$K_{\pm}^{yQ}(u,v) = \frac{1}{2}\Big(K_{yQ}(u,v) \mp K_Q(u-v)\Big)\,. \tag{A.9}$$

Further important kernels entering the $Y_\pm$ related TBA-type equations are defined as follows:

$$K_{xv}^{QM}(u,v) = \frac{1}{2\pi i}\frac{d}{du}\log S_{xv}^{QM}(u,v)\,,$$

$$S_{xv}^{QM}(u,v) = \frac{x(u - i\frac{Q}{g}) - x(v + i\frac{M}{g})}{x(u + i\frac{Q}{g}) - x(v + i\frac{M}{g})}\frac{x(u - i\frac{Q}{g}) - x(v - i\frac{M}{g})}{x(u + i\frac{Q}{g}) - x(v - i\frac{M}{g})}\frac{x(u + i\frac{Q}{g})}{x(u - i\frac{Q}{g})}$$

$$\times \prod_{j=1}^{M-1}\frac{u - v - \frac{i}{g}(Q - M + 2j)}{u - v + \frac{i}{g}(Q - M + 2j)}\,. \tag{A.10}$$

The kernels entering the right hand sides of the equation (2.9) for Y_1 are

$$
\begin{aligned}
K_{vwx}^{QM}(u,v) &= \frac{1}{2\pi i}\frac{d}{du}\log S_{vwx}^{QM}(u,v)\,,\\
S_{vwx}^{QM}(u,v) &= \frac{x(u-i\frac{Q}{g})-x(v+i\frac{M}{g})}{x(u-i\frac{Q}{g})-x(v-i\frac{M}{g})}\frac{x(u+i\frac{Q}{g})-x(v+i\frac{M}{g})}{x(u+i\frac{Q}{g})-x(v-i\frac{M}{g})}\frac{x(v-i\frac{M}{g})}{x(v+i\frac{M}{g})}\\
&\times\prod_{j=1}^{Q-1}\frac{u-v-\frac{i}{g}(M-Q+2j)}{u-v+\frac{i}{g}(M-Q+2j)}\,,
\end{aligned}\tag{A.11}
$$

and the dressing-phase related kernel $K_{\mathfrak{sl}(2)}^{QM}(u,v)$, which is built from the $\mathfrak{sl}(2)$ S-matrix of the model [49]. It is of the form

$$
S_{\mathfrak{sl}(2)}^{QM}(u,v)=S^{QM}(u-v)^{-1}\,\Sigma_{QM}(u,v)^{-2}\,,\tag{A.12}
$$

where Σ^{QM} is the improved dressing factor [50]. The corresponding $\mathfrak{sl}(2)$ and dressing kernels are defined in the usual way

$$
K_{\mathfrak{sl}(2)}^{QM}(u,v)=\frac{1}{2\pi i}\frac{d}{du}\log S_{\mathfrak{sl}(2)}^{QM}(u,v)\,,\quad K_{QM}^{\Sigma}(u,v)=\frac{1}{2\pi i}\frac{d}{du}\log\Sigma_{QM}(u,v)\,.\tag{A.13}
$$

Explicit expressions for the improved dressing factors $\Sigma_{QM}(u,v)$ can be found in section 6 of ref. [50]. Here for our numerical computations we used the single integral representation given in [21].

Finally we mention that along the lines of [42] in the derivation of the formula (2.10) for $\Omega(\mathcal{K}_Q)$, it was exploited that all the necessary kernels: $K_Q, K_{Qy}, K_{xv}^{Q1}, s\star K_{vwx}^{Q-1,1}, K_{y1}, K_{\mathfrak{sl}(2)}^{Q1}$ satisfy the identity:

$$
\mathcal{K}_Q - s\star\mathcal{K}_{Q-1} - s\star\mathcal{K}_{Q+1}\equiv\delta\mathcal{K}_Q = 0,\qquad\text{for}\quad Q\geq 3.\tag{A.14}
$$

B Kernel matrices of the vertical HNLIE part

In this appendix the kernel matrices appearing in the upper HNLIE part of our equations (2.18,2.19) are presented. Here the kernel matrices are different compared to those published in [38]. The difference comes simply from a reformulation the equations in the language of new unknown functions. In [38] the unknowns are 6 b-type functions:

$$
\underline{b}^{\mathrm{old}}=\{b_{1,s}^{(3)[\gamma_1]},b_{2,s}^{(3)[\gamma_2]},b_{3,s}^{(3)[\gamma_3]},b_{1,s}^{(2)[-1+\gamma_4]},b_{2,s}^{(2)[-1+\gamma_5]},b_{1,s}^{(1)[-2+\gamma_6]}\},\tag{B.1}
$$

and 6 d-type functions:

$$\underline{d}^{\text{old}} = \{d_{1,s}^{(3)[\eta_1]}, d_{2,s}^{(3)[\eta_2]}, d_{3,s}^{(3)[\eta_3]}, d_{1,s}^{(2)[\eta_4]}, d_{2,s}^{(2)[\eta_5]}, d_{1,s}^{(1)[\eta_6]}\}, \tag{B.2}$$

with shift vectors $\underline{\gamma}$ and $\underline{\eta}$ given by (2.20,2.21). We recognized that the kernels become simpler if we formulate the equations in terms of the unknowns:

$$\underline{b} = \{b_{1,s}^{(3)[\gamma_1]}, \eta/b_{2,s}^{(3)[\gamma_2]}, b_{3,s}^{(3)[\gamma_3]}, \eta/b_{1,s}^{(2)[-1+\gamma_4]}, b_{2,s}^{(2)[-1+\gamma_5]}, b_{1,s}^{(1)[-2+\gamma_6]}\}, \tag{B.3}$$

and

$$\underline{d} = \{d_{1,s}^{(3)[\eta_1]}, \eta/d_{2,s}^{(3)[\eta_2]}, d_{3,s}^{(3)[\eta_3]}, d_{1,s}^{(2)[\eta_4]}, \eta/d_{2,s}^{(2)[\eta_5]}, d_{1,s}^{(1)[\eta_6]}\}, \tag{B.4}$$

where $\eta = \pm 1$ is a global sign factor and $s = p_0$, if one adopts the notation of [38] for the HNLIE equations (2.18,2.19). Another advantage of using the variables (B.3,B.4) is that they are either $O(1)$ or exponentially small for large volumes.

For the sake of simplicity, here we give the form of the kernels of (2.18,2.19) before the application of the contour shifts (2.20,2.21). The kernels of the equations can be obtained from these by simply shifting their arguments according to the formulas below:

$$
\begin{aligned}
G_{bB}(u)_{ab} &= K_{bB}\left(u + \frac{i}{g}(\gamma_a - \gamma_b)\right)_{ab}, & a,b &= 1,...,6 \\
G_{bD}(u)_{ab} &= K_{bD}\left(u + \frac{i}{g}(\gamma_a - \eta_b)\right)_{ab}, & a,b &= 1,...,6 \\
G_{dB}(u)_{ab} &= K_{dB}\left(u + \frac{i}{g}(\eta_a - \gamma_b)\right)_{ab}, & a,b &= 1,...,6 \\
G_{dD}(u)_{ab} &= K_{dD}\left(u + \frac{i}{g}(\eta_a - \eta_b)\right)_{ab}, & a,b &= 1,...,6.
\end{aligned}
\tag{B.5}
$$

The kernel matrices can be expressed by the functions as follows[27]:

$$G(u) = \frac{g}{8\pi}\left\{\psi(1 + \frac{i\,g\,u}{4}) + \psi(1 - \frac{i\,g\,u}{4}) - \psi(\frac{1}{2} + \frac{i\,g\,u}{4}) - \psi(\frac{1}{2} + \frac{i\,g\,u}{4})\right\}, \tag{B.6}$$

$$l(u) = \frac{g}{8\pi}\left\{\psi(1 + \frac{i\,g\,u}{4}) + \psi(1 - \frac{i\,g\,u}{4})\right\}, \tag{B.7}$$

$$s(u) = \frac{g}{4}\frac{1}{\cosh(\frac{\pi g u}{2})} \tag{B.8}$$

---

[27] $\psi(z) = \frac{d}{dz}\log\Gamma(z)$.

and they take the form:

$$
K_{bB} = \begin{pmatrix}
G & 0 & G - s^+ & -s & s^+ - G & 0 \\
0 & l & 0 & l - s^- & s & 0 \\
G - s^- & 0 & G & 0 & s^- - G & 0 \\
s & l - s^+ & 0 & l & 0 & s \\
s^- - G & -s & s^+ - G & 0 & G & s^- \\
0 & 0 & 0 & -s & s^+ & G
\end{pmatrix},
\qquad (\text{B}.9)
$$

$$
K_{bD} = \begin{pmatrix}
-G & 0 & s^+ - G & G - s^+ & 0 & 0 \\
0 & -l & 0 & -s & s^+ - l & 0 \\
s^- - G & 0 & -G & G - s^- & s & 0 \\
-s & s^+ - l & 0 & 0 & s^+ - l & s \\
G - s^- & s & G - s^+ & -G & 0 & s^- \\
0 & 0 & 0 & s^- & -s & -G^{--}
\end{pmatrix},
\qquad (\text{B}.10)
$$

$$
K_{dB} = \begin{pmatrix}
-G & 0 & s^+ - G & s & G - s^+ & 0 \\
0 & -l & 0 & s^- - l & -s & 0 \\
s^- - G & 0 & -G & 0 & G - s^- & 0 \\
G - s^- & s & G - s^+ & 0 & -G & s^+ \\
0 & s^- - l & -s & s^- - l & 0 & s \\
0 & 0 & 0 & -s & s^+ & -G^{++}
\end{pmatrix},
\qquad (\text{B}.11)
$$

$$
K_{dD} = \begin{pmatrix}
G & 0 & G - s^+ & s^+ - G & 0 & 0 \\
0 & l & 0 & s & l - s^+ & 0 \\
G - s^- & 0 & G & s^- - G & -s & 0 \\
s^- - G & -s & s^+ - G & G & 0 & s^+ \\
0 & l - s^- & s & 0 & l & s \\
0 & 0 & 0 & s^- & -s & G
\end{pmatrix}.
\qquad (\text{B}.12)
$$

38

C   Asymptotic solutions of the vertical HNLIE

In this section along the lines of [38] the asymptotic solutions of the upper $SU(4)$ NLIE variables are presented . In the asymptotic limit the T-hook of AdS/CFT splits into two $SU(2|2)$ fat-hooks. The basic building blocks of the asymptotic solution are the nine Q-functions corresponding to the left and right $SU(2|2)$ fat-hooks. Due to the left-right symmetry of the Y-system it is enough to give the right Q-functions. They can be derived from the asymptotic solution of the Y-functions given in [4]. They take the form:

$$
\begin{aligned}
&Q^{(2,2)}(u) = q_{22}, && Q^{(1,2)}(u) = g\,\Lambda\,q_{11}\,\sigma(u)\,u^{+}, && Q^{(0,2)}(u) = 4\,g\,u^{++}, \\
&Q^{(2,1)}(u) = \frac{2\,q_{22}}{g\,\Lambda\,u^{-}}, && Q^{(1,1)}(u) = q_{11}\,\sigma(u), && Q^{(0,1)}(u) = \frac{2}{\Lambda}, \\
&Q^{(2,0)}(u) = \frac{4\,q_{22}\,u^{--}}{g\,u^{-}\,u^{---}} && Q^{(1,0)}(u) = \Lambda\,q_{11}\,\sigma(u), && Q^{(0,0)}(u) = 1,
\end{aligned}
\tag{C.1}
$$

where q_{11}, q_{22} and Λ are arbitrary constants which cancel from the final form of the asymptotic NLIE variables. Furthermore $\sigma(u) = e^{\frac{\pi\,g\,u}{2}}$ to satisfy the recursion $\frac{\sigma^{+}}{\sigma^{-}} = -1$. The further building blocks of the asymptotic solution are as follows:[28]

$$
T_{s,1} = \frac{4\,(-1)^{s}\,s\,u}{u^{[s]}},
\tag{C.2}
$$

and

$$
\mathcal{A}^{o}(u) = \frac{4\,u}{g\,u^{+}\,u^{-}}, \qquad \mathcal{B}^{o}(u) = 4\,g\,u, \qquad \beta^{o}(u) = \frac{2\,\sigma^{-}(u)}{\Lambda}, \qquad \gamma^{o}(u) = \frac{2\,\sigma(u)}{g\,\Lambda\,u}.
\tag{C.3}
$$

The solution of the recursions

$$
w^{o-} - w^{o+} = \frac{\mathcal{A}^{o}}{\gamma^{o+}\gamma^{o-}}, \qquad\qquad y^{o+} - y^{o-} = \frac{\mathcal{B}^{o}}{\beta^{o}\beta^{o--}},
\tag{C.4}
$$

are as follows:

$$
w^{o}(u) = -\frac{i\,\Lambda^{2}\,e^{-\pi\,g\,u}}{4}((g\,u)^{2} + w_{c}), \qquad\qquad y^{o}(u) = \frac{i\,\Lambda^{2}\,e^{-\pi\,g\,u}}{4}((g\,u)^{2} + w_{c} - i\,C),
\tag{C.5}
$$

---

[28] Here for correspondence we use the same letters for the names of different unknowns as in [38].

where w_c and C are arbitrary constants. Using the building blocks listed above, the asymptotic form of the upper $SU(4)$ NLIE functions can be determined [38] and take the form:

$$b_{1,s}^{(3)o}(u) = b_{3,s}^{(3)o}(u) = \frac{s\, u^+}{u^{[-s]}}, \tag{C.6}$$

$$B_{1,s}^{(3)o}(u) = B_{3,s}^{(3)o}(u) = \frac{(s+1)\, u}{u^{[-s]}}, \tag{C.7}$$

$$b_{2,s}^{(3)o}(u) = B_{2,s}^{(3)o}(u) = -\phi^{[-s]}(u)\,\frac{1}{4\, g\, s\, u}, \tag{C.8}$$

$$b_{1,s}^{(2)o-}(u) = B_{1,s}^{(2)o-}(u) = \frac{\phi^{[-s]}(u)}{4\, g\, s\, u + C}, \tag{C.9}$$

$$b_{2,s}^{(2)o-}(u) = -\frac{C + 4\, g\, s\, u^-}{4\, g\, u^{[-s]}}, \qquad B_{2,s}^{(2)o-}(u) = -\frac{C + 4\, g\, (s-1)\, u}{4\, g\, u^{[-s]}}, \tag{C.10}$$

$$b_{1,s}^{(1)o--}(u) = \frac{C + 4\, g\, (s-1)\, u}{4\, g\, u^{[-s]}}, \qquad B_{1,s}^{(1)o--}(u) = \frac{C + 4\, g\, s\, u^-}{4\, g\, u^{[-s]}}, \tag{C.11}$$

$$d_{1,s}^{(3)o}(u) = d_{3,s}^{(3)o}(u) = \frac{s\, u^-}{u^{[s]}}, \tag{C.12}$$

$$D_{1,s}^{(3)o}(u) = D_{3,s}^{(3)o}(u) = \frac{(s+1)\, u}{u^{[s]}}, \tag{C.13}$$

$$d_{2,s}^{(3)o}(u) = D_{2,s}^{(3)o}(u) = -\frac{1}{\phi^{[s]}(u)}\,\frac{(g\, u^{[s]})^2}{4\, g\, s\, u}, \tag{C.14}$$

$$d_{1,s}^{(2)o}(u) = -\frac{C + 4\, g\, s\, u^+}{4\, g\, u^{[s]}}, \qquad D_{1,s}^{(2)o}(u) = -\frac{C + 4\, g\, (s-1)\, u}{4\, g\, u^{[s]}}, \tag{C.15}$$

$$d_{2,s}^{(2)o}(u) = D_{2,s}^{(2)o}(u) = -\frac{\phi^{[s]}(u)\, (g\, u^{[s]})^2}{4\, g\, s\, u + C}, \tag{C.16}$$

$$d_{1,s}^{(1)o}(u) = \frac{C + 4\, g\, (s-1)\, u}{4\, g\, u^{[s]}}, \qquad D_{1,s}^{(1)o}(u) = \frac{C + 4\, g\, s\, u^+}{4\, g\, u^{[s]}}, \tag{C.17}$$

where s is the "cutoff index" where the TBA $\to$ HNLIE replacements starts[29], furthermore for any index distribution B^o and D^o stand for $1 + b^o$ and $1 + d^o$ respectively.

$$\phi(u) = \frac{x(u)^{2L}}{g\, u}, \tag{C.18}$$

and C is the arbitrary constant that does not cancel from the formula for the HNLIE variables. The asymptotic solution for the six b- and d-type NLIE-functions of the

---

[29]In section 2. it is denoted by p_0, here the notation s is kept to fit to formulas of [38].

system can be obtained from the Bäcklund functions above by appropriately shifting their arguments:

$$\mathbf{b}^o = \{b_a^o\} = \{b_{1,s}^{(3)o[\gamma_1]}, \eta/b_{2,s}^{(3)o[\gamma_2]}, b_{3,s}^{(3)o[\gamma_3]}, \eta/b_{1,s}^{(2)o[-1+\gamma_4]}, b_{2,s}^{(2)o[-1+\gamma_5]}, b_{1,s}^{(1)o[-2+\gamma_6]}\},$$
$$\text{(C.19)}$$

$$\mathbf{d}^o = \{d_a^o\} = \{d_{1,s}^{(3)o[\eta_1]}, \eta/d_{2,s}^{(3)o[\eta_2]}, d_{3,s}^{(3)o[\eta_3]}, d_{1,s}^{(2)o[\eta_4]}, d_{2,s}^{(2)o[\eta_5]}, d_{1,s}^{(1)o[\eta_6]}\}, \qquad \text{(C.20)}$$

with the shifts given in (2.20,2.21). Finally we note that the $C = 0$ choice implies a symmetry relation between the b- and d-type variables. Let $\mathfrak{M}$ the 6 by 6 matrix:

$$\mathfrak{M} = \begin{pmatrix} 0 & 0 & 1 & 0 & 0 & 0 \\ 0 & 1 & 0 & 0 & 0 & 0 \\ 1 & 0 & 0 & 0 & 0 & 0 \\ 0 & 0 & 0 & 0 & 1 & 0 \\ 0 & 0 & 0 & 1 & 0 & 0 \\ 0 & 0 & 0 & 0 & 0 & 1 \end{pmatrix}. \qquad \text{(C.21)}$$

Then at $C = 0$ the $\mathbf{b}^o$ and $\mathbf{d}^o$ vectors satisfy the relations as follows:

$$\mathbf{d}^o(u) = \mathfrak{M}\mathbf{b}^o(-u), \qquad \mathbf{b}^o(-u) = \mathbf{b}^{o*}(u), \qquad \text{(C.22)}$$

$$\mathbf{d}^o(u) = \mathfrak{M}\mathbf{b}^{o*}(u), \qquad \mathbf{d}^o(-u) = \mathbf{d}^{o*}(u), \qquad \text{(C.23)}$$

where $*$ denotes complex conjugation. In our numerical studies we mostly use the $C = 0$ asymptotic solution to setup the equations to solve. In this case the exact equations guarantee the fulfillment of (2.22), which reduces to 6 the number of independent complex functions of the upper NLIE part.

D Asymptotic solutions of the Y-system and the horizontal $SU(2)$-type HNLIE

This appendix is devoted to give the asymptotic solution for the Y-functions and the variables of the horizontal $SU(2)$ NLIE. The asymptotic form of the Y-functions can be read off from the asymptotic T-functions in [4]. They take the form:

$$Y_{m|vw}^o(u) = \frac{m(m+2)\, g^2\, u^2}{(m+1)^2 + g^2\, u^2}, \quad m = 1, 2, \dots \qquad \text{(D.1)}$$

$$Y_Q^o(u) = \left(\frac{1}{x_s^{[Q]}(u)\, x_s^{[-Q]}(u)}\right)^{2L} \frac{16\, Q^2\, g^2\, u^2}{g^2\, u^2 + Q^2}, \qquad Q = 1, 2, \ldots \tag{D.2}$$

$$Y_-^o(u) = Y_+^o(u) = -\frac{g^2\, u^2}{2 + g^2\, u^2}, \tag{D.3}$$

$$Y_{1|w}^o(u) = \frac{g^2\, u^2\, (19 + 3\, g^2\, u^2)}{(1 + g^2 u^2)(4 + g^2 u^2)}. \tag{D.4}$$

Following the lines of [38] the asymptotic horizontal $SU(2)$ NLIE variables can be determined from the asymptotic Q-functions (C.1). Here we just list the final formulas:

$$b^o(u) = b_0(u - i\,\gamma), \qquad \bar{b}^o(u) = \bar{b}_0(u + i\,\gamma), \tag{D.5}$$

where

$$b_0(u) = \frac{2\,(g^2\, u^2 - 3\,i)\,(1 + 2\,i\,g\,u + g^2\, u^2)}{(g^2\, u^2 + i)\,(g^2\, u^2 - 2\,i)\,(g^2\, u^2 + 3\,i)}, \tag{D.6}$$

$$\bar{b}_0(u) = \frac{2\,(g^2\, u^2 + 3\,i)\,(1 - 2\,i\,g\,u + g^2\, u^2)}{(g^2\, u^2 - i)\,(g^2\, u^2 + 2\,i)\,(g^2\, u^2 - 3\,i)}, \tag{D.7}$$

and $0 < \gamma < 1/2$ is the arbitrary contour shift parameter of the horizontal $SU(2)$ NLIE.

References

[1] J. M. Maldacena, *"The large N limit of superconformal field theories and supergravity,"* Adv. Theor. Math. Phys. **2** (1998) 231, [*Int. J. Theor. Phys.* **38** (1999) 1113];

[2] S. S. Gubser, I. R. Klebanov and A. M. Polyakov, *"Gauge theory correlators from non-critical string theory,"* Phys. Lett. B **428** (1998) 105;

[3] E. Witten, *"Anti-de Sitter space and holography,"* Adv. Theor. Math. Phys. **2** (1998) 253;

[4] Z. Bajnok, N. Drukker, Á. Hegedűs, R. I. Nepomechie, L. Palla, C. Sieg, R. Suzuki, *"The spectrum of tachyons in AdS/CFT"* JHEP **1403** (2014) 055.

[5] N. Beisert, C. Ahn, L. F. Alday, Z. Bajnok, J. M. Drummond, L. Freyhult, N. Gromov and R. A. Janik *et al.*, *"Review of AdS/CFT Integrability: An Overview,"* Lett. Math. Phys. **99** (2012) 3.

[6] O. DeWolfe and N. Mann, *Integrable open spin chains in defect conformal field theory*, JHEP **0404** (2004) 035,

[7] D. Berenstein and S. E. Vazquez, *Integrable open spin chains from giant gravitons*, JHEP **0506** (2005) 059,

[8] D. M. Hofman and J. M. Maldacena, *Reflecting magnons*, JHEP **0711** (2007) 063,

[9] D. Correa and C. Young, *Reflecting magnons from D7 and D5 branes*, J.Phys.A **A41** (2008) 455401,

[10] D. H. Correa, V. Regelskis, and C. A. Young, *Integrable achiral D5-brane reflections and asymptotic Bethe equations*, J.Phys.A **A44** (2011) 325403,

[11] Z. Bajnok and R. A. Janik, *"Six and seven loop Konishi from Luscher corrections,"* JHEP **1211** (2012) 002

[12] S. Leurent, D. Serban and D. Volin, *"Six-loop Konishi anomalous dimension from the Y-system,"* Phys. Rev. Lett. **109** (2012) 241601

[13] S. Leurent and D. Volin, *"Multiple zeta functions and double wrapping in planar N = 4 SYM,"* Nucl. Phys. B **875** (2013) 757

[14] C. Marboe, D. Volin, *"Quantum spectral curve as a tool for a perturbative quantum field theory"* `arXiv:1411.4758`.

[15] C. Marboe, V. Velizhanin and D. Volin, *"Six-loop anomalous dimension of twist-two operators in planar N=4 SYM theory,"* arXiv:1412.4762 [hep-th].

[16] N. Gromov, *"Y-system and Quasi-Classical Strings,"* JHEP **1001** (2010) 112.

[17] N. Gromov, V. Kazakov and Z. Tsuboi, *"PSU(2, 2|4) Character of Quasiclassical AdS/CFT,"* JHEP **1007** (2010) 097

[18] Z. Bajnok, M. Kim and L. Palla, *"Spectral curve for open strings attached to the Y=0 brane,"* JHEP **1404** (2014) 035

[19] N. Gromov, F. Levkovich-Maslyuk, G. Sizov and S. Valatka, *"Quantum spectral curve at work: from small spin to strong coupling in $\mathcal{N} = 4$ SYM,"* JHEP **1407** (2014) 156

[20] N. Gromov, V. Kazakov and P. Vieira, *"Exact Spectrum of Planar $\mathcal{N} = 4$ Supersymmetric Yang-Mills Theory: Konishi Dimension at Any Coupling,"* Phys. Rev. Lett. **104** (2010) 211601

[21] S. Frolov, *Konishi operator at intermediate coupling, J.Phys.* **A44** (2011) 065401,

[22] S. Frolov, *"Scaling dimensions from the mirror TBA,"* J. Phys. A **45** (2012) 305402.

[23] J. McGreevy, L. Susskind, and N. Toumbas, *Invasion of the giant gravitons from Anti-de Sitter space, JHEP* **0006** (2000) 008,

[24] V. Balasubramanian, M. Berkooz, A. Naqvi, and M. J. Strassler, *Giant gravitons in conformal field theory, JHEP* **0204** (2002) 034,

[25] V. Balasubramanian, M.-x. Huang, T. S. Levi, and A. Naqvi, *Open strings from $\mathcal{N} = 4$ superYang-Mills, JHEP* **0208** (2002) 037,

[26] A. LeClair, G. Mussardo, H. Saleur, and S. Skorik, *Boundary energy and boundary states in integrable quantum field theories*, *Nucl.Phys.* **B453** (1995) 581–618,

[27] D. Correa and C. Young, *Finite size corrections for open strings/open chains in planar AdS/CFT*, *JHEP* **0908** (2009) 097,

[28] L. Palla, *Yangian symmetry of boundary scattering in AdS/CFT and the explicit form of bound state reflection matrices*, *JHEP* **1103** (2011) 110,

[29] C. Ahn and R. I. Nepomechie, *Yangian symmetry and bound states in AdS/CFT boundary scattering*, *JHEP* **1005** (2010) 016,

[30] N. Drukker, *Integrable Wilson loops*, *JHEP* **1310** (2013) 135,

[31] D. Correa, J. Maldacena, and A. Sever, *The quark anti-quark potential and the cusp anomalous dimension from a TBA equation*, *JHEP* **1208** (2012) 134,

[32] Z. Bajnok, J. Balog, D. H. Correa, Á. Hegedűs, F. I. Schaposnik Massolo and G. Zsolt Tóth, *"Reformulating the TBA equations for the quark anti-quark potential and their two loop expansion,"* *JHEP* **1403** (2014) 056,

[33] N. Gromov, V. Kazakov and P. Vieira, *"Integrability for the Full Spectrum of Planar AdS/CFT,"* *Phys.Rev.Lett.* **103:131601**,2009,

[34] D. Bombardelli, D. Fioravanti and R. Tateo, *"Thermodynamic Bethe Ansatz for planar AdS/CFT: A Proposal,"* J. Phys. A **42** (2009) 375401

[35] G. Arutyunov and S. Frolov, *"Thermodynamic Bethe Ansatz for the $AdS_5 \times S^5$ Mirror Model,"* JHEP **0905** (2009) 068

[36] A. Cavaglia, D. Fioravanti, and R. Tateo, *Extended Y-system for the AdS_5/CFT_4 correspondence*, *Nucl.Phys.* **B843** (2011) 302–343,

[37] J. Balog and A. Hegedus, *"$AdS_5 \times S^5$ mirror TBA equations from Y-system and discontinuity relations,"* JHEP **1108** (2011) 095

[38] J. Balog, Á. Hegedűs, *"Hybrid-NLIE for the AdS/CFT spectral problem"* JHEP **1208** (2012) 022.

[39] Z. Bajnok and L. Palla, *Boundary finite size corrections for multiparticle states and planar AdS/CFT*, JHEP **1101** (2011) 011,

[40] G. Arutyunov, S. Frolov, R. Suzuki, *"String hypothesis for the $AdS_5 \times S^5$ mirror"* JHEP**03** (2009) 152.

[41] G. Arutyunov, S. Frolov, R. Suzuki, *"Exploring the mirror TBA"* JHEP **05** (2010) 031.

[42] J. Balog, Á. Hegedűs, *"Quasi-local formulation of the mirror TBA"* JHEP **1205** (2012) 039.

[43] R. Suzuki, *"Hybrid NLIE for the mirror $AdS_5 \times S^5$ "* J.Phys.**A44** (2011) 235401.

[44] C. Destri and H. J. de Vega, *"Nonlinear integral equation and excited states scaling functions in the sine-Gordon model,"* Nucl. Phys. B **504** (1997) 621-644

[45] A. Hegedus, *"Finite size effects and 2-string deviations in the spin-1 XXZ chains,"* J. Phys. A **40** (2007) 12007

[46] N. Gromov, V. Kazakov, S. Leurent and D. Volin, *"Solving the AdS/CFT Y-system,"* JHEP **1207** (2012) 023

[47] N. Gromov, V. Kazakov, S. Leurent and D. Volin, *"Quantum Spectral Curve for Planar $\mathcal{N} =$ Super-Yang-Mills Theory,"* Phys. Rev. Lett. **112** (2014) 1, 011602

[48] N. Gromov, V. Kazakov, S. Leurent, D. Volin, *Quantum spectral curve for arbitrary state/operator in AdS_5/CFT_4* `arXiv:1405.4857`.

[49] G. Arutyunov and S. Frolov, *"Foundations of the $AdS_5 \times S^5$ Superstring. Part I,"* J. Phys. A **42** (2009) 254003

[50] G. Arutyunov, S. Frolov, *"The dressing factor and crossing equations"*, J. Phys. A **42**, 425401 (2009)